UNITED NATIONS UNIVERSITY
GEOTHERMAL TRAINING PROGRAMME

ORKUSTOFNUN

Strokkur geyser, Haukadalur

Andi J. Nugroho

OPTIMIZATION OF ELECTRICAL POWER PRODUCTION FROM HIGH-TEMPERATURE GEOTHERMAL FIELDS WITH RESPECT TO SILICA SCALING PROBLEMS

Report 2
December 2011

UNITED NATIONS UNIVERSITY
GEOTHERMAL TRAINING PROGRAMME
Orkustofnun, Grensásvegur 9,
IS-108 Reykjavík, Iceland

Reports 2011
Number 2

OPTIMIZATION OF ELECTRICAL POWER PRODUCTION FROM HIGH-TEMPERATURE GEOTHERMAL FIELDS WITH RESPECT TO SILICA SCALING PROBLEMS

MSc thesis
School of Engineering and Natural Sciences
Faculty of Mechanical Engineering
University of Iceland

by

Andi J. Nugroho
Pertamina Geothermal Energy
Kamojang
INDONESIA
andi.nugroho@pertamina.com - andijoko@pge.pertamina.com

United Nations University
Geothermal Training Programme
Reykjavík, Iceland
Published in December 2011

ISBN 978-9979-68-303-2
ISSN 1670-7427

This MSc thesis has also been published in May 2011 by the
School of Engineering and Natural Sciences
Faculty of Industrial Engineering, Mechanical Engineering and Computer Science
University of Iceland

INTRODUCTION

The Geothermal Training Programme of the United Nations University (UNU) has operated in Iceland since 1979 with six month annual courses for professionals from developing countries. The aim is to assist developing countries with significant geothermal potential to build up groups of specialists that cover most aspects of geothermal exploration and development. During 1979-2011, 482 scientists and engineers from 50 developing countries have completed the six month courses. They have come from Asia (41%), Africa (30%), Central America (16%), and Central and Eastern Europe (13%). There is a steady flow of requests from all over the world for the six month training and we can only meet a portion of the requests. Most of the trainees are awarded UNU Fellowships financed by the Government of Iceland and the UNU.

Candidates for the six month specialized training must have at least a BSc degree and a minimum of one year practical experience in geothermal work in their home countries prior to the training. Many of our trainees have already completed their MSc or PhD degrees when they come to Iceland, but several excellent students who have only BSc degrees have made requests to come again to Iceland for a higher academic degree. In 1999, it was decided to start admitting UNU Fellows to continue their studies and study for MSc degrees in geothermal science or engineering in co-operation with the University of Iceland. An agreement to this effect was signed with the University of Iceland. The six month studies at the UNU Geothermal Training Programme form a part of the graduate programme.

It is a pleasure to introduce the 27th UNU Fellow to complete the MSc studies at the University of Iceland under the co-operation agreement. Mr. Andi Joko Nugroho, BSc in Mechanical Engineering, of PT Pertamina Geothermal Energy, Indonesia, completed the six month specialized training in Geothermal Utilization at the UNU Geothermal Training Programme in October 2007. His research report was entitled: " Evaluation of waste brine utilization from LHD Unit III for electricity generation in Lahendong geothermal field, Indonesia". After two years of geothermal research work in Indonesia, he came back to Iceland for MSc studies at the Faculty of Earth Sciences of the University of Iceland in August 2009. In May 2011, he defended his MSc thesis presented here, entitled " Optimization of electrical power production from high-temperature geothermal fields with respect to silica scaling problems ". His studies in Iceland were financed by the Government of Iceland through a UNU-GTP Fellowship from the UNU Geothermal Training Programme. We congratulate him on his achievements and wish him all the best for the future. We thank the Faculty of Industrial Engineering, Mechanical Engineering and Computer Science at the School of Engineering and Natural Sciences of the University of Iceland for the co-operation, and his supervisors for the dedication.

Finally, I would like to mention that Andi Joko's MSc thesis with the figures in colour is available for downloading on our website *www.unugtp.is* under publications.

With warmest wishes from Iceland,

Ingvar B. Fridleifsson, director
United Nations University
Geothermal Training Programme

ACKNOWLEDGEMENTS

I would like to express my sincerest gratitude to the Government of Iceland through the United Nations University Geothermal Training Programme (UNU-GTP) for sponsoring my Master of Science studies at the University of Iceland, and to PT. Pertamina Geothermal Energy for supporting and permitting me to attend this MSc study. I am very grateful to Dr. Ingvar Birgir Fridleifsson, the director of UNU-GTP, and Mr. Lúdvík S. Georgsson, the deputy director of UNU-GTP, for giving me the opportunity to attend the programme. Special thanks go to the staff of UNU GTP: Thórhildur Ísberg, Dorthe H. Holm, Ingimar Gudni Haraldsson and Markús A.G. Wilde for their outstanding assistance during my stay in Iceland.

I am indebted to my supervisors, Associate Professor Halldór Pálsson and Professor Magnús Thór Jónsson for their guidance and support during all stages of this work. I wish to express my appreciation to Professor Páll Valdimarsson for reviewing this thesis with valuable comments.

Finally, I would like to express my deepest appreciation to my family for their moral support.

ABSTRACT

Silica scaling is an obstacle in the use of geothermal fluid from high-temperature fields. The potential issue of silica deposition rises with increasing resource temperature. A single flash condensing system is the most common energy conversion system for utilizing geothermal fluid from high-temperature fields, mainly due to its smallest possibility of silica precipitation. This thesis investigates the possibility of optimizing the employment of geothermal fluid from high-temperature fields by using an alternative energy conversion system in place of a conventional single flash cycle with a condensing turbine.

Thermodynamic and silica scaling calculations were modelled and simulated in Matlab for five different energy conversion systems in order to obtain the optimum specific power output for each power conversion system. The models include: a single flash and a double flash condensing system, a combination of a single flash condensing cycle and a binary cycle utilizing separated brine, a combination of a single flash back pressure cycle and a binary cycle utilizing the turbine exhaust steam, and a combination of a single flash back pressure cycle and a binary cycle utilizing both separated brine and exhaust steam. An economical analysis was also performed to find the total capital investment needed for different energy conversion systems at their optimum power output production. The specific power outputs and total capital investments for different power conversion systems were finally compared.

Results from the study show that the employment of geothermal fluid from a high-temperature field at a certain range of fluid enthalpy and resource temperature could be optimized by using the double flash system, the combination of a single flash condensing cycle and a binary cycle, or the combination of a single flash back pressure cycle and a binary cycle. These results can be used by a decision maker to identify the most appropriate energy conversion system for making use of geothermal fluid from high-temperature fields where silica scaling becomes a hindrance based on a given geothermal fluid enthalpy and resource temperature.

TABLE OF CONTENTS

LIST OF FIGURES

LIST OF TABLES

1. INTRODUCTION

Geothermal energy could be a viable solution for reducing the effects of global warming and dependence on fossil fuel, since the availability of geothermal energy is potentially enormous. The interest in developing geothermal energy has been increasing as a consequence of rising oil prices. Geothermal energy can be used for electricity generation and direct uses depending on the temperature and chemistry of the resources. Electricity power production is the most important utilization of geothermal energy from high-temperature geothermal resources.

Geothermal fluid must be cooled to as low a temperature as possible in order to achieve maximum conversion of geothermal energy into electricity. In many cases, the geothermal fluid becomes supersaturated with silica as it is cooled. Silica scaling potential can be estimated from the reservoir temperature. Hotter resource temperatures will lead to higher silica saturation in the disposal brine, the consequences of which could lead to the possibility of greater silica scaling precipitation in reinjection wells, piping, heat exchangers and other production facilities. The potential seriousness of silica deposition problems for various types of resources and for selected types of power plants can be estimated by using correlations between the equilibrium solubility of quartz and amorphous silica (DiPippo, 1985).

There are several different types of power conversion systems which can be used for electricity generation from geothermal energy. The most common energy conversion systems are single flash, double flash, binary cycle and combinations of flash systems and binary cycle systems. A single flash condensing cycle is the most common energy conversion system for utilizing geothermal fluid due to its simple construction and to the resultant low possibility of silica precipitation. The total installed capacity in the world for each type of power plant is: single flash plants 42.2%, dry steam plants 26%, double flash plants 23%, binary plants 3.9%, combined flash and binary plants 3.8%, triple flash 1% and hybrid plants 0.06% (DiPippo, 2007). A double flash cycle can produce 15-25% more power output than a single flash condensing cycle for the same geothermal fluid conditions (DiPippo, 2007).

For high-temperature resources, combinations of single flash cycles using a back-pressure turbine with binary cycles, using either separated brine or exhaust steam from the back pressure turbine, can better utilize the geothermal fluid. This configuration is often called a hybrid system.

The optimization of maximum power output per unit mass flow of geothermal fluid was studied previously by using the interaction between an optimization routine in Matlab and the thermodynamics database in Engineering Equation Solver (EES) (Karlsdóttir, 2008). Another study about the optimization of possible bottoming units for a single flash plant was done by using the thermodynamic database Refprop 8.0 with a global optimization method (Bandoro Svandaru, 2009). These two researches did not include the effect of silica scaling in the optimization process.

This thesis investigates the possibility of optimizing the utilization of geothermal fluid from high-temperature fields where silica scaling has become the most important constraint. Five types of an energy conversion system were modelled:

- Single flash condensing system
- Double flash condensing system
- Combination of a single flash condensing cycle and a binary cycle utilizing the separated brine. This plant configuration is called a "brine bottoming binary system" for simplification of the term.
- Combination of a single flash back pressure cycle and a binary cycle utilizing exhaust steam from the back pressure unit. This plant configuration is called a "spent steam bottoming binary system".
- Combination of a single flash back pressure cycle, a binary cycle utilizing separated brine and a binary cycle utilizing exhaust steam from the back pressure unit. This plant configuration is called a "hybrid system".

The discharge enthalpy of wells producing from liquid-dominated reservoirs is not always the same as the saturated liquid enthalpy at reservoir temperature. It is often higher than the saturated liquid enthalpy. Based on analytical data on water and steam samples collected at the wellhead, there are several reasons for the excess enthalpy of well discharges (Arnórsson, 2005):

- The presence of a significant fraction of steam in the initial reservoir fluid.
- The production wells have multiple feed zones, vapour-dominated at shallow depth and deep liquid-dominated feed zones.
- Depressurization in the producing reservoirs as a consequence of production causes cooling of the reservoir fluid, thus creating conductive heat transfer from rock to fluid, increasing the fluid enthalpy.
- Depressurization in the reservoirs causes phase segregation, where the water and steam phases in the depressurization zone partly separate due to their different flow properties. Adhesive forces between mineral surfaces and fluid, which are the cause of capillary pressure, are stronger for water than for steam, thus reducing the mobility of the liquid and increasing the steam fraction.

Due to the variability of well discharge enthalpy with reservoir temperatures, two different cases are considered:

- Geothermal fluid is produced from wells with no excess enthalpy
  In this case the discharge enthalpy of wells is the same as the enthalpy of saturated liquid at the reservoir temperature. The range of the reservoir temperature to be simulated is from 200 to 300°C.
- Geothermal fluid is produced from wells with excess enthalpy
  In this case the discharge enthalpy of wells is higher than the enthalpy of saturated liquid at the reservoir temperature. The range of the reservoir temperature to be simulated is from 240 to 300°C and the range of the fluid enthalpy is from 1400 to 2200 kJ/kg.

From the simulation the following data can be determined:

- Expected net power output per unit mass flow;
- Design variables which give the maximum net power output;
- Total capital investment;
- Most appropriate energy conversion system for utilizing geothermal fluid from high-temperature field.

The results can be used by a decision maker to identify the most appropriate energy conversion system for utilizing geothermal fluid from high-temperature fields based on given geothermal fluid enthalpy and resource temperature. Another objective is to determine the expected specific net power output per unit mass flow of geothermal fluid as well as the optimum design variables which would give maximum power output, and the total investment cost for each type of energy conversion system.
The structure of the thesis is as follows:

Chapters 2 and 3 contain the basic theories about thermodynamic models for different power cycle types (single flash, double flash, combined and hybrid system) and the estimation of silica scaling based on reservoir temperatures.
Chapter 4 presents the economical analysis.
Chapter 5 describes the model-based reasoning, design variables, constraints and general assumptions.
Chapter 6 presents the results of the optimization such as the optimum expected net power output, optimum operation parameters, total capital investment costs and a comparison of the different power cycles.
Chapter 7 provides the findings of this thesis.

2. ENERGY CONVERSION SYSTEM

2.1 Single flash system

In two-phase high-temperature fields, geothermal fluid from a reservoir reaches the surface as a mixture of steam and brine due to boiling of the fluid. The steam is then separated from the brine, either by a cyclone effect in a vertical separator or by gravity in a horizontal separator. The dry steam is directed to a turbine which is connected to a generator to generate electricity while the separated brine is piped back into the reservoir through reinjection wells. According to the type of turbine (exhaust condition of the turbine), this system can be divided into two types:

a. Single flash condensing system

Figure 2.1 shows a simplified schematic diagram for the single flash system with a condensing turbine. Steam exiting the turbine is directed to a condenser operating at vacuum pressure. Low vacuum pressure in the condenser is maintained in order to increase the enthalpy difference in the turbine as well as to increase the power output of the plant. Non condensable gasses, associated with steam which is accumulated in the condenser, potentially increase the condenser pressure and must, therefore, be pumped out of the condenser. Vacuum pumps, steam jet ejectors or compressors are installed for that purpose. In this model, the gasses are assumed to be extracted from a condenser by using a compressor. In direct contact condensers, cooling water from a cooling tower is typically sprayed at the top of the condenser, condensing the steam back into liquid form. The mixture of condensate and cooling water is then pumped to the top of the cooling tower for heat rejection to the environment.

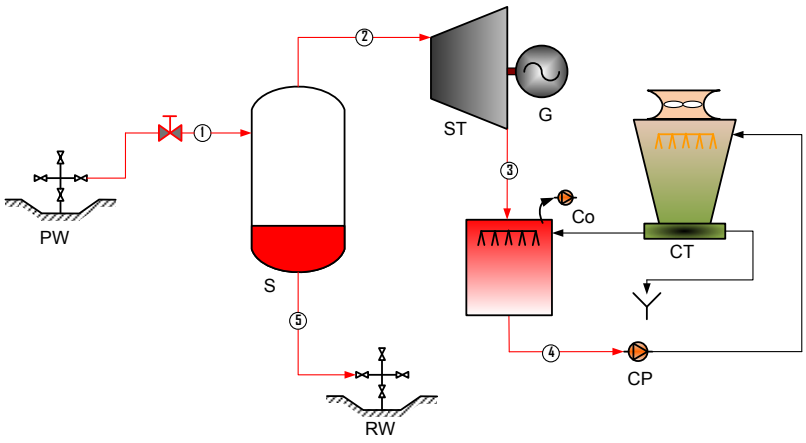

FIGURE 2.1: Simplified schematic diagram of a single flash condensing system

The temperature-entropy diagram of a single flash condensing system is shown in Figure 2.2. The process starts with geothermal fluid at reservoir conditions which is pressurized and generally close to the liquid-saturation state (point 0). Decreasing the pressure by means of a throttle valve will cause the geothermal fluid to be flashed and produce a mixture of steam and brine. It can be assumed with enough accuracy that the flashing process is isenthalpic because heat losses from the well to the surroundings are very small compared to the energy flow upwards. Also, there is no work involved and changes in the kinetic and potential energy can be neglected. The result is:

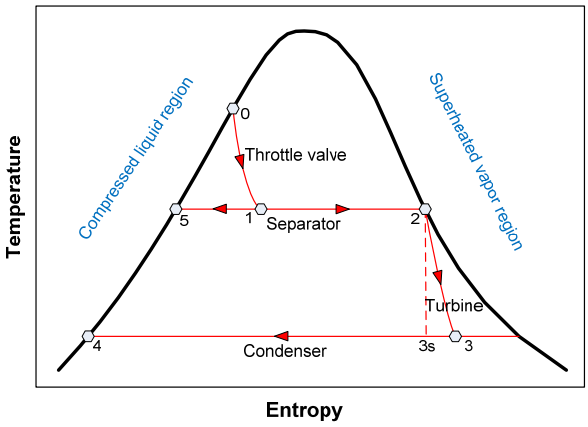

FIGURE 2.2: Temperature-entropy diagram of a single flash condensing system

$$h_1 = h_0 \tag{2.1}$$

The mass fraction of the mixture at state 1, x_1 can be calculated from:

$$x_1 = \frac{h_1 - h_5}{h_2 - h_5} \tag{2.2}$$

where h_5 and h_2 are the saturated liquid enthalpy and the saturated steam enthalpy at separator pressure.

The mass flow of dry steam, $\dot{m}_3$ and separated brine, $\dot{m}_5$ are found from:

$$\dot{m}_3 = x_1 \dot{m}_1 \tag{2.3}$$

$$\dot{m}_5 = (1 - x_1)\dot{m}_1 \tag{2.4}$$

The power output of the turbine is calculated from:

$$\dot{W}_t = \dot{m}_3(h_2 - h_3) \tag{2.5}$$

The enthalpy at turbine outlet, h_3 is calculated by solving:

$$\eta_t = \frac{h_2 - h_3}{h_2 - h_{3s}} \tag{2.6}$$

where η_t is the isentropic efficiency of a turbine.

The isentropic efficiency of a turbine is affected by the amount of moisture that is present during the expansion process. This effect can be quantified by using the Baumann rule, which states that 1% average moisture causes roughly a 1% drop in turbine efficiency. Since geothermal steam turbines usually operate in the wet region, the degradation in performance must be considered (DiPippo, 2007). Adopting the Baumann rule, the isentropic efficiency for a turbine operating with wet steam is given by:

$$\eta_t = \eta_{td} \cdot \left[\frac{x_{inlet} + x_{outlet}}{2}\right] \tag{2.7}$$

In this case, the isentropic efficiency of a turbine is defined as:

$$\eta_t = \eta_{td} \cdot \left[\frac{x_2 + x_3}{2}\right] \tag{2.8}$$

where the dry turbine efficiency, η_{td} may be conservatively assumed to be constant at 85%.
The net power output of a single flash system is calculated by subtracting the power output of the turbine with auxiliary power consumption for a cooling-water pump, a compressor for NCG removal and a cooling tower fan.

b. Single flash back pressure system

Figure 2.3 shows a simplified schematic diagram of a single flash system with a back pressure unit. This term "back pressure" is used because the exhaust pressure of the turbine is much higher than the condensing system. The system does not use a condenser. The outlet steam from the turbine exhausts directly to the atmosphere or returns to the plant for heating purposes. In this process the exhaust pressure is controlled by a regulating valve to suit the needs of the process steam pressure. The steam consumption per power output from a back pressure turbine is almost double that from the condensing type at the same inlet pressure.

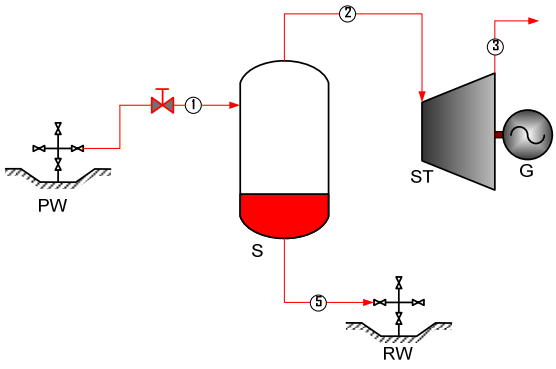

FIGURE 2.3: Simplified schematic diagram of a single flash back pressure

2.2 Double flash system

Figure 2.4 shows a simplified schematic diagram of a double flash system. This configuration is very similar to a single flash system. The double flash system uses a two stage separation of geothermal

fluid instead of one, resulting in two steam admission pressures at the turbine. First, the geothermal fluid from the well is flashed at relatively high pressure. Steam and brine are separated in the separator. From the separation process, the resulting high pressure steam is directed to a high pressure turbine and the separated brine, which still contains reasonably high enthalpy, is throttled and directed to a low pressure separator for additional steam production. Steam from the high pressure turbine is mixed with the steam from the low pressure separator and then directed to the low pressure turbine to generate extra power. The brine from a low pressure separator is piped to the reinjection wells. The silica concentration of the brine injected into the reinjection wells becomes higher in the double flash system, when compared to a single flash one, and could result in scaling problems in the pipelines or the reinjection wells.

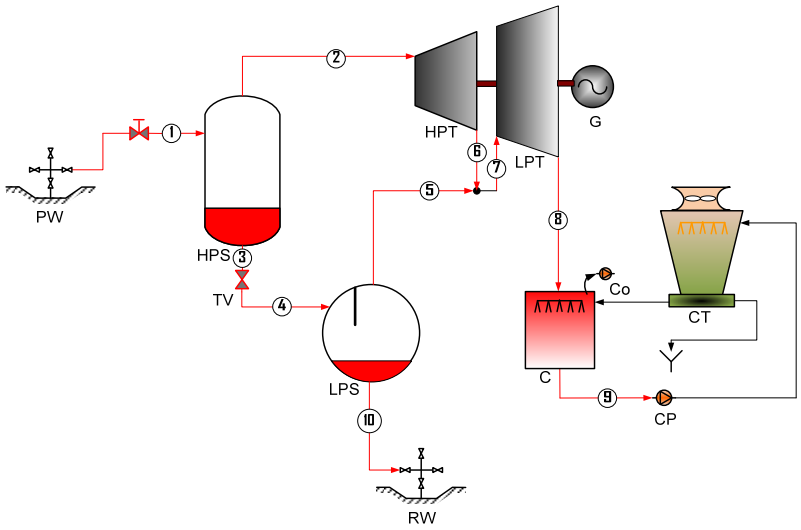

FIGURE 2.4: Simplified schematic diagram of a double flash system

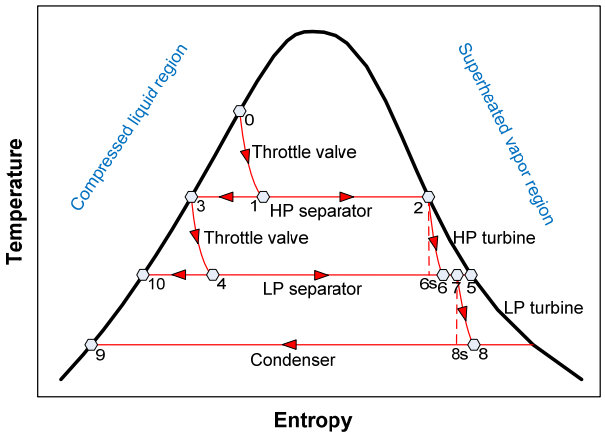

FIGURE 2.5: Temperature-entropy diagram of a double flash system

The processes are best described in a thermodynamic temperature-entropy diagram as shown in Figure 2.5. The hot separated brine at the saturation liquid state (point 3) is flashed by means of a throttle valve and produces a low-pressure mixture of steam and brine. The flashing process is isenthalpic, therefore:

$$h_3 = h_4 \tag{2.9}$$

The low-pressure steam mass flow, $\dot{m}_5$ is found from

$$\dot{m}_5 = x_4 \dot{m}_4 \tag{2.10}$$

where the mass fraction of the mixture at state 4, x_4 can be calculated from:

$$x_4 = \frac{h_4 - h_{10}}{h_5 - h_{10}} \tag{2.11}$$

The dry steam from the low-pressure separator is then mixed with the exhaust steam from a high-pressure turbine before entering the low pressure turbine, thus:

$$\dot{m}_7 = \dot{m}_5 + \dot{m}_6 \tag{2.12}$$

$$h_7 = \frac{\dot{m}_5 h_5 + \dot{m}_6 h_6}{\dot{m}_7} \tag{2.13}$$

The power generated with high-pressure and low-pressure turbines in a double flash system is derived from:

$$\dot{W}_{HPt} = \dot{m}_2 (h_2 - h_6) \tag{2.14}$$

$$\dot{W}_{LPt} = \dot{m}_7 (h_7 - h_8) \tag{2.15}$$

where isentropic efficiencies of a high-pressure turbine, η_{HPt} and a low-pressure turbine, η_{LPt} are calculated from:

$$\eta_{HPt} = \eta_{td} \cdot \left[\frac{x_2 + x_6}{2}\right] \quad (2.16)$$

$$\eta_{LPt} = \eta_{td} \cdot \left[\frac{x_7 + x_8}{2}\right] \quad (2.17)$$

The net power output of a double flash system is calculated by summing up the power output of the turbines (HP turbine and LP turbine) and subtracting auxiliary power consumption for the cooling-water pumps, compressors for NCG removal and the cooling tower fans.

2.3 Combined cycle system

In a combined single flash cycle and binary cycle, the heat from hot separated brine or exhaust steam from the back-pressure steam turbine is transferred to a secondary binary fluid. In this thesis, three configurations of combined cycles are considered.

a. Brine bottoming binary (BBB) system

A brine bottoming binary (BBB) system is a combination of a single flash cycle using a condensing turbine and a binary cycle as a bottoming unit. The system is shown schematically in Figure 2.6. The dry steam from the separator is directed to a condensing steam turbine. Steam exiting the turbine is directed to a condenser operating at vacuum pressure. The hot separated brine which still contains high enthalpy is utilized to vaporize the working fluid in the binary cycle and thus produce additional power output.

The working fluid is selected by considering the critical temperature and pressure for optimizing power output of the plant. The following table shows the critical temperature (T_c) and the critical pressure (P_c) of some common working fluids for binary plants.

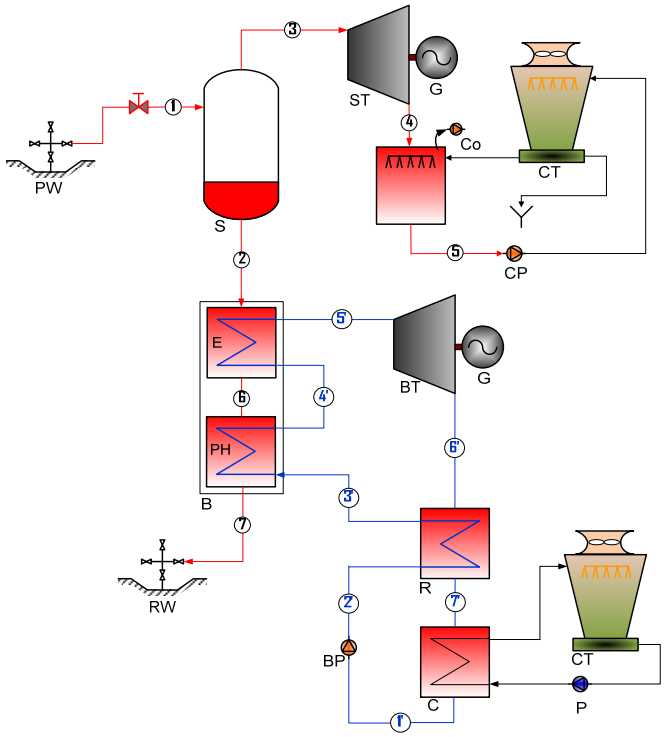

FIGURE 2.6: Simplified schematic diagram of a BBB system

TABLE 2.1: Properties of organic working fluids (DiPippo, 2007)

Working fluid	Formula	Molar mass	T_c (°C)	P_c (bar)
isobutane	i-C_4H_{10}	58.12	135.92	36.85
n-butane	C_4H_{10}	58.12	150.8	37.18
isopentane	i-C_5H_{12}	72.15	187.8	34.09
n-pentane	C_5H_{12}	72.15	193.9	32.4

The working fluid absorbs heat from a heat source, in this case the hot brine, via shell and tube heat exchangers. This heat causes the working fluid to evaporate, producing the high pressure vapour that is then expanded through a turbine which is connected to a generator. The exhaust vapour from the low

pressure turbine is then condensed using either air-cooled or water-cooled shell and tube heat exchangers. In this case, a water-cooled system coupled with a wet cooling tower is used. From the condenser, the liquid working fluid is pumped to a high pressure and returned to the boiler to close the cycle. Due to silica scaling which limits the excess brine temperature, it is feasible to incorporate an additional heat exchanger into the cycle, known as a recuperator. In a recuperator, residual sensible heat in the low-pressure turbine exhaust stream is used for initial preheating of the cold liquid from the feed pump.

A temperature-enthalpy diagram of a brine bottoming binary system is shown in Figure 2.7. The mass flow of the binary fluid, $\dot{m}_{wf}$ is found from the energy balance in the boiler:

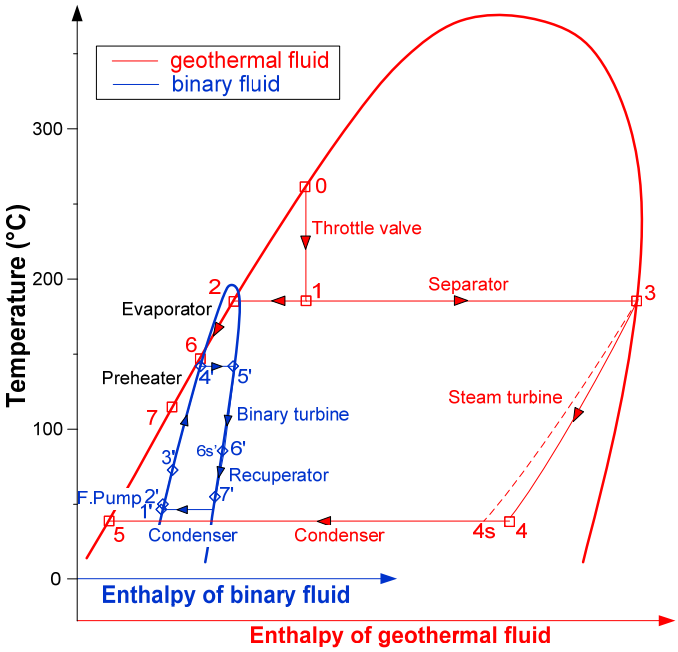

FIGURE 2.7: Temperature-enthalpy diagram of a BBB system with n-pentane as the ORC fluid

$$\dot{m}_{brine}(h_2 - h_7) = \dot{m}_{wf}(h_{5'} - h_{3'}) \quad (2.18)$$

The power output of the binary turbine, $\dot{W}_{ORC}$ is calculated by assuming an adiabatic process, negligible potential and kinetic energy as:

$$\dot{W}_{ORC} = \dot{m}_{wf}(h_{5'} - h_{6'}) = \dot{m}_{wf}.\eta_t.(h_{5'} - h_{6s'}) \quad (2.19)$$

where the binary turbine efficiency, η_t may be conservatively assumed to be 85% because of dry expansion in the turbine.

The net power output of a BBB system is calculated by summing up the power output of the turbines (steam turbine and binary turbine) and subtracting the auxiliary power consumption of binary fluid pumps, cooling-water pumps, compressors for NCG removal and cooling tower fans.

b. Spent steam bottoming binary (SSBB) system

A spent steam bottoming binary (SSBB) system is a combination of a single flash cycle using a back pressure turbine and a binary cycle. A SSBB system is very suitable for utilizing geothermal fluid containing high non condensable gasses which make it n to use a condensing turbine. The system is shown schematically in Figure 2.8. The dry steam from the separator is directed to a back-pressure steam turbine. Steam exiting the turbine is then condensed in the pre-heater and the evaporator of the binary cycle. Thus, condensation heat of the steam is used to vaporize the working fluid in the binary cycle.

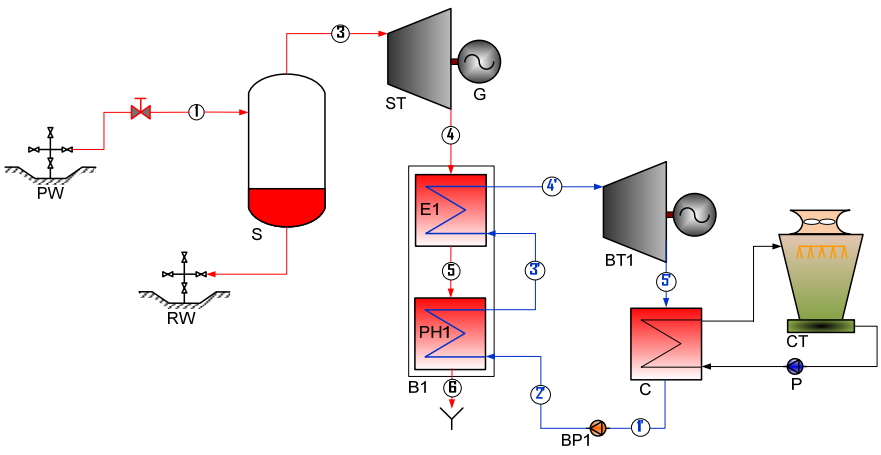

FIGURE 2.8: Simplified schematic diagram of a SSBB system

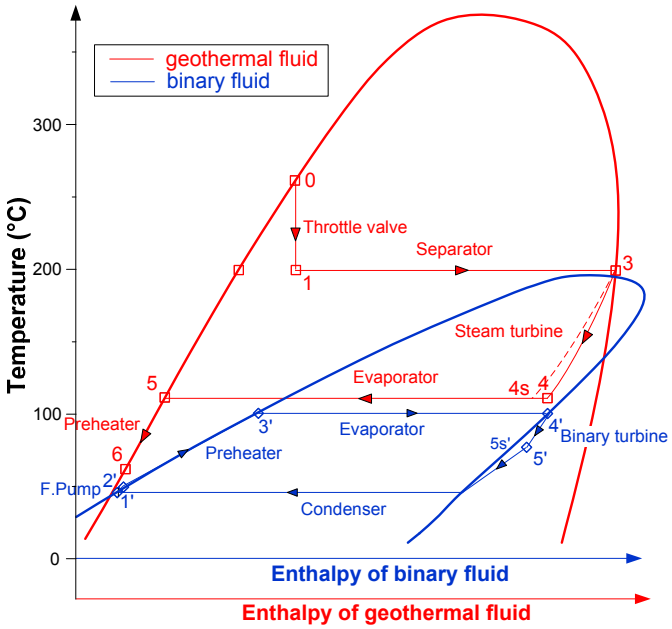

FIGURE 2.9: Temperature-enthalpy diagram of a SSBB system

A condenser for the binary cycle shown in Figure 2.8 is a water-cooled condenser, but an air-cooled condenser is a better choice if there are not enough water supplies at plant site. The temperature-enthalpy diagram of a SSBB system is shown in Figure 2.9. The net power output of a SSBB system is calculated by summing up the power output of the turbines (steam turbine and binary turbine) and subtracting the auxiliary power consumption of binary fluid pumps, cooling-water pumps and cooling tower fans.

c. Hybrid system

Basically, a hybrid system is a combination of a SSBB system and a BBB system. This plant configuration consists of a single flash back pressure cycle, a binary cycle utilizing separated brine and a binary cycle utilizing the exhaust steam from the back pressure unit, as shown schematically in Figure 2.10. The dry steam first powers the back-pressure steam turbine and is then condensed in the boiler of the first binary cycle. The separated brine is used to preheat and evaporate the working fluid in the second binary cycle.

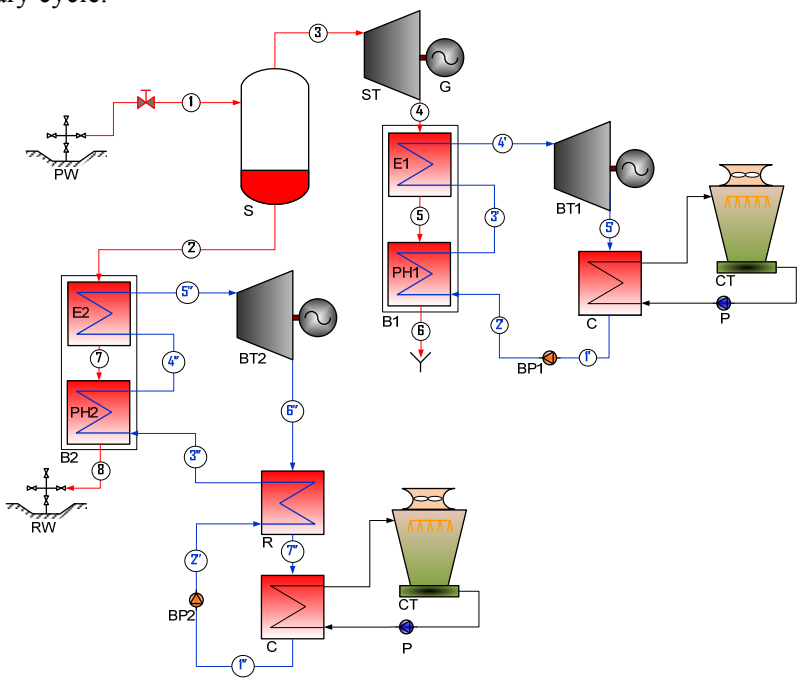

FIGURE 2.10: Simplified schematic diagram of a hybrid system

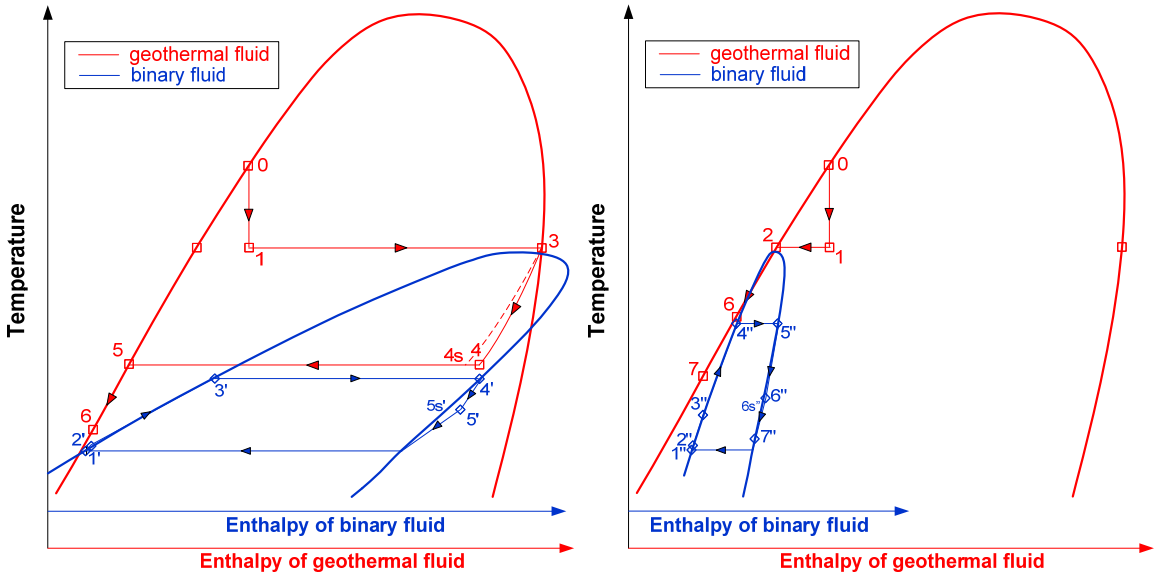

a. Steam-powered ORC *b. Brine-powered ORC*

FIGURE 2.11: Temperature-enthalpy diagram of a hybrid system

A temperature-enthalpy diagram of a hybrid system is shown in Figure 2.11. The net power output of a hybrid system is calculated by summing up the power output of the turbines (steam turbine and binary turbines) and subtracting the auxiliary power consumption for binary fluid pumps, cooling-water pumps and cooling tower fans.

This plant configuration is used for example in the 125 MW Upper Mahiao plant in the Philippines, the 100 MW Mokai I and Mokai II plants in New Zealand and the 30 MW Puna plant in Hawaii (Bronicki, 2008).

3. ESTIMATING SILICA SCALING POTENTIAL

The states of silica are crystalline and noncrystalline (also called amorphous). Crystalline silica can take several forms: quartz, cristobalite, tridymite, and four other rare forms. The differences between each form are in the arrangement of individual atoms that form the crystal lattice for each mineral. Quartz and amorphous silica are the forms related to the silica scaling problem in geothermal systems. Generally, the geothermal fluid in the reservoir will be in equilibrium with quartz. Flashing or cooling the geothermal fluid will make the fluid become saturated with respect to quartz. Fortunately, the precipitation of silica at lower temperatures is controlled by amorphous silica equilibrium which is more soluble than quartz.

A method for estimating the silica scaling potential in geothermal power plants was given by DiPippo (1985). The paper describes calculations for estimating silica scaling potential in flashing and binary systems, based on the reservoir temperature and the temperature of the discharge brine.

3.1 Equilibrium quartz solubility

In the reservoir, geothermal fluid is assumed to be in equilibrium with respect to dissolved quartz. As described by DiPippo (1985), the correlation between reservoir temperature, t(°C) and quartz concentration for zero salinity, q_0 (ppm) is:

$$t = -42.198 + 0.28831 \cdot q_0 - 3.6686 \cdot 10^{-4} \cdot {q_o}^2 + 3.1665 \cdot 10^{-7} \cdot {q_o}^3 + 77.034 \cdot \log(q_o) \quad (3.1)$$

This correlation is valid over a range of temperatures from 20°C to 330°C.

A correction due to the effects of salinity on quartz solubility (q) is expressed as:

$$q = q_0 \cdot [1 - 0.2 \cdot m(1 - 0.3363 \cdot t^{0.1644})] \quad (3.2)$$

where q_0 is zero salinity solubility (ppm), t is the reservoir temperature (°C) and m is reservoir salinity (molal NaCl).

3.2 Silica concentration in flashing and binary systems

The silica remains in the liquid phase. Therefore, after the flashing process of the geothermal fluid, the silica concentration will increase in the separated hot water due to the removal of the steam fraction. In the single flash case, the silica concentration (s_{sf}) will increase according to:

$$s_{sf} = \frac{q}{(1 - x_1)} \quad (3.3)$$

where, x_1 is a steam quality at flashing pressure.

The geothermal fluid has non zero salinity and, therefore, x_1 in Equation 3.3 is corrected to be:

$$x_1 = \frac{h_f(t_r, c_r) - h_f(t_1, c_1)}{h_g(t_1) - h_f(t_1, c_1)} \quad (3.4)$$

where, t_1 is the flashing temperature, c_r is the salt concentration in the reservoir and c_1 is the salt concentration in the separated liquid.

The salt concentration in the separated liquid is given by:

$$c_1 = \frac{c_r}{(1 - x_1)} \quad (3.5)$$

where the value of x_1 is determined iteratively from Equations 3.4 and 3.5.

In the double flash case, the silica concentration in the separated hot water is according to:

$$s_{db} = \frac{q}{(1 - x_1) \cdot (1 - x_2)} \tag{3.6}$$

where, x_2 is the steam quality at the second flashing pressure.

For non zero salinity, x_2 in Equation 3.6 is corrected to be:

$$x_2 = \frac{h_f(t_1, c_1) - h_f(t_2, c_2)}{h_g(t_2) - h_f(t_2, c_2)} \tag{3.7}$$

where t_2 is the temperature of the second stage flash and c_2 is the salt concentration in the liquid from the second stage flash.

The salt concentration in the liquid from the second stage flash is given by:

$$c_2 = \frac{c_1}{(1 - x_2)} \tag{3.8}$$

where the value of x_2 is determined iteratively from Equations 3.7 and 3.8.

In a binary system, the geothermal fluid is maintained in the liquid phase and therefore the silica concentration is constant during the cooling process:

$$s_b = q \tag{3.9}$$

where s_b is the silica concentration in a binary system.

3.3 Equilibrium amorphous silica solubility

The equilibrium solubility of amorphous silica for zero salinity s_0 (ppm), according to the equation (DiPippo, 1985), is:

$$\log(s_o) = -6.116 + 0.01625 \cdot T - 1.758 \cdot 10^{-5} \cdot T^2 + 5.257 \cdot 10^{-9} \cdot T^3 \tag{3.10}$$

where s_0 is amorphous silica concentration at zero salinity in ppm and T is the absolute temperature of discharge brine in K.

Amorphous silica and quartz concentrations at zero salinity as a function of reservoir temperature are shown in Figure 3.1.

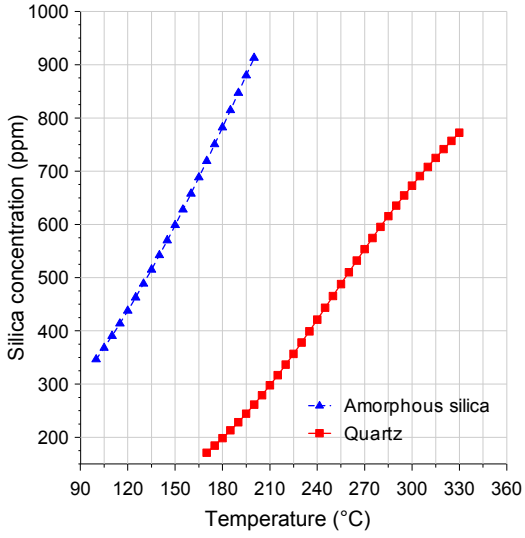

FIGURE 3.1: Amorphous silica and quartz concentrations at zero salinity as a function of reservoir temperature

The correlation in Equation 3.10 is valid for temperatures between 90°C and 340ºC. A correction to this zero-salinity solubility is given by:

$$s_{eq} = s_0 \cdot 10^{-m \cdot D} \tag{3.11}$$

where m is reservoir salinity (molal NaCl).

The value of D is calculated from:

$$\log(D) = -1.0569 - 1.573 \cdot 10^{-3} t \tag{3.12}$$

where t is the temperature of the discharge brine in C.

The correlations in Equations 3.11 and 3.12 are valid for temperatures between 25 and 300°C.

3.4 Silica Saturation Index (SSI)

To determine whether silica will tend to precipitate or not, the values of the silica concentration after flashing or cooling is compared with the equilibrium amorphous silica concentration, given as the ratio:

$$SSI = \frac{s}{s_{eq}} \tag{3.13}$$

If the silica concentration after flashing or cooling is higher than equilibrium solubility of amorphous silica (SSI > 1), then silica will tend to precipitate and there is a risk of silica scaling in the surface equipment, reinjection wells and reservoir. In many geothermal fields, as described in this section, the kinetics of the formation of solid silica deposits are rather slow and therefore the actual limit for SSI would probably be higher than the estimation.

The Rotokawa geothermal field in New Zealand operates without any silica problems, combining a back-pressure and a binary system based on the SSI value of 1.4 (result of mixing brine with condensate). The Kawarau field, also located in New Zealand, operates a binary system based on the SSI value of 1.4-1.5 in discharge brine, without any treatment of the brine. The Mak-Ban field in the Philippines operates a bottoming cycle using ORC and has introduced an acid treatment (bringing down the pH level from 6.3 to 5.5) to reduce the silica polarization rate at a SSI value of 1.7 (Grassiani, 1999). In the Palinpinon-I geothermal field in the Philippines, the SSI was monitored and maintained at 1.2 to prevent silica deposition (Jordan et al., 2000).

Based on the previous experience of the geothermal fields described above, the limit value of SSI assumed for this analysis is 1.2 instead of 1. The SSI is used as a constraint for fluid utilization from high-temperature fields.

4. ECONOMICAL ANALYSIS

Economical assessment is an analytical tool used to evaluate the viability of a future investment. Based on the power plant design, an estimate of the total capital cost can be performed. A more complex level in the power plant design could give additional power output but this could require more equipment and, as consequence, higher investment cost. Therefore, economic factors are important considerations in power plant design selection. One purpose of an economical analysis is to compare the total capital investment cost and the total power production for each plant design in order to optimize the income from the power production. The power plant design requiring the smallest total capital investment to generate a fixed amount of electricity is the best option.

The total capital investment is estimated based on the purchased equipment cost (PEC), the installation and construction cost, and the cost of the geothermal fluid.

4.1 Purchased equipment cost

The purchased equipment cost (PEC) is calculated based on the size and the price of the individual pieces of equipment in the power plant. The size of the equipment was estimated in the same phase as the thermodynamic optimization. The purchase costs for different types of turbines are shown in Table 4.1.

TABLE 4.1: Purchase costs for different turbine types

Turbine type	Purchased cost US$/kW	Reference
Single flash - back pressure	540	EPA, 2002
Single flash - condensing	912.5	Reyman, 2000
Double flash	958	GEA, 2005
Binary	725	Hjartarson, 2009
	750	Lukawski, 2009

Reyman (2000) states that the price of a condensing steam turbine is strongly influenced by the power production capacity of the unit. The proposed price for a turbine size ranging from 110 MW units to 55 MW is from US$850/kW to US$1000/kW. The average price for this range, US$ 912.5/kW, is used for the condensing turbine estimation cost in this study. The price of a back-pressure turbine was based on information from TurboSteam Inc. for 500 kW which was commercially available in 2002 (EPA, 2002). The price of a double flash steam turbine is estimated assuming that the average capital cost of a double flash power plant is 5% more than the average capital cost of single flash technology (GEA, 2005).

Probability distributions are used in the input parameters of the cost model. This is done since many prices are suggested in the literature. A normal distribution with a standard deviation of 5% for the unit price is applied for both the single flash and the double flash turbine.

Unlike a steam turbine, the binary turbine has a limited maximum production capacity size. Common sizes for binary turbines are between 2 and 5 MW. Larger power production is usually achieved by using a series of small binary turbine unit. Therefore, the power plant size does not have a higher influence in the cost of binary turbines. A uniform distribution in the range of 725 US$/kW to 750 US$/kW is applied for the binary turbine price.

Purchase costs for heat exchangers, separators, compressors, pumps and cooling tower fans, as shown in Equations 4.1 to 4.7, are calculated using correlations given by Seider (2003). Basic cost (C_B) for shell and tube heat exchangers is given by non-linear equations in which the heat exchanger area is used as a variable. The basic cost for a boiler (kettle vaporizer model) is:

$$C_B = \exp\{11.967 - 0.8709 \cdot \ln(A) + 0.09005 \cdot [\ln(A)]^2\} \quad (4.1)$$

Recuperator and condenser (fixed head model) costs are calculated using:

$$C_B = \exp\{11.0545 - 0.9228 \cdot \ln(A) + 0.09861 \cdot [\ln(A)]^2\} \quad (4.2)$$

where A is the heat exchanger area in ft^2. The equation is valid for the range of heat exchanger areas between 150 and 12000 ft^2.

The cost of heat exchangers is determined by taking into consideration materials, dimensions and a pressure factor according to:

$$C_P = F_P F_M F_L C_B \quad (4.3)$$

where F_M is the material factor for combinations of tube and shell material, F_L is the tube length correction factor and F_P represents the shell-side pressure factor.

The cost of separators (vertical type), C_P, including nozzles, manholes, support and ladders is calculated using:

$$C_P = \exp\{6.775 + 0.181255 \cdot \ln(W) + 0.02297 \cdot (\ln(W))^2\} \cdot F_M + 285.1 \cdot D_i^{0.7396} \cdot L^{0.70684} \quad (4.4)$$

where W is the weight of vessel in lbs, D_i is the inside diameter in ft, L is the height in ft and F_M is a material factor. Weight and dimension of a separator are calculated based on the international standard for pressure vessels. The equation is valid for $4200 < W < 1000000$ lb, $3 < Di < 21$ ft and $12 < L < 40$ ft.

The purchase cost of compressors for NCG removal includes driver couplings and electric motors, and is calculated according to:

$$C_B = \exp\{7.2223 + 0.8 \cdot \ln(Pc)\} \quad (4.5)$$

For the pumps, the correlation is:

$$C_B = \exp\{5.4866 + 0.1314 \cdot \ln(Pp) + 0.053255 \cdot (\ln(Pp))^2 + 0.028628 \cdot (\ln(Pp))^3 - 0.0035549 \cdot (\ln(Pp))^4\} + \exp\{7.3883 + 0.26986 \cdot \ln(Pp) + 0.06718 \cdot (\ln(Pp))^2\} \quad (4.6)$$

where Pc is the compressor power and Pp is the pump power, in horsepower (hp) units.

The purchase cost of the cooling tower fans includes driver couplings and electric motors, and is calculated using:

$$C_B = \exp\{6.6547 + 0.79 \cdot \ln(Pc)\} \quad (4.7)$$

Those correlations mentioned above are based on the equipment cost in the middle of year 2000. The cost generally escalates with time due to inflation. Therefore, the values should be adjusted to the reference year of 2010 using e.g. the Chemical Engineering (CE) Plant Cost Index, where the value should be increased by 34% in order to get the current price.

The cost of wet cooling towers is calculated using the online cost estimator available at the website of Cooling Tower Depot (2010). A scaling exponent was used in order to compensate for differences in the size of the cooling tower load, affecting the price of a cooling tower by the relation (Bejan, 1996):

$$C_{B,Y} = C_{B,X} \left(\frac{Q_{CT,Y}}{Q_{CT,X}} \right)^{0.6} \quad (4.8)$$

where Q_{CT} is the heat load of a cooling tower.

4.2 Remaining total capital investment

The installation and construction costs can be estimated from the purchased equipment cost, as shown in Table 4.2 (Bejan, 1996).

TABLE 4.2: The installation and construction costs

Cost components	Value
Purchased-equipment installation	20% of PEC
Piping	20% of PEC
Instrumentation and controls	10% of PEC
Electrical equipment and materials	10% of PEC
Civil, structural and architectural work	20% of PEC
Engineering and supervision	20% of PEC

The drilling cost per unit well depth is estimated at 800-1200 US$/m (Barbier, 2002). Other references state that drilling cost can be estimated using the following correlation (GEA, 2005):

$$Drilling\ cost = 240785 + 210 \cdot well\ depth + 0.019069 \cdot (well\ depth)^2 \qquad (4.9)$$

where the drilling cost is in US$ and well depth is in ft. Using the correlation in Equation 4.9, drilling cost can be estimated as 1220 US$/m for 2 km deep wells. Average mass flow rate from production wells is assumed to be 19 kg/s (average value in Lahendong geothermal field, Indonesia). The specific cost of geothermal fluid is estimated by dividing the drilling cost of 2 km deep geothermal wells, with the average of the total mass flow from the Lahendong field. In this case, the specific production cost of the geothermal fluid is 128000 US$ per unit mass flow, or $ / (kg/s).

A normal distribution with a standard deviation of 5% unit price was applied to account for the uncertain drilling cost per meter, uncertain well depth and the uncertain average total mass flow from the wells.

5. OPTIMIZATION OF SPECIFIC POWER OUTPUT

5.1 Model-based reasoning

The thermodynamic model equations of the power plants as well as the silica scaling calculations were modelled in Matlab. The thermodynamic properties of the fluid database, called Refprop, were used in Matlab.

The optimization method used in this analysis process, is a direct search method called grid search. This method involves setting up a suitable grid in the design space, evaluating the objective function at all the grid points, and finding the grid point corresponding to the lowest function value (Rao, 1996). This optimization method is used in Matlab, which also evaluates thermodynamic properties and solves the system of equations.

An optimization of the power plant model is done in order to find the maximum specific net power output for each power cycle. The specific power output is calculated for unit mass flow from the production wells. The unit of specific power output is kW/(kg/s), or kJ/kg. The design variables related to maximum power output are used as an input to the model. Any variation of design variables were simulated to obtain the output of specific power output. Afterwards, constraints are applied to ensure a legal solution in a thermodynamical sense and to take into account the design limitations.
The optimization process in this analysis used these basic steps:

- Design a thermodynamic model for the power cycle;
- Define the design variables and the constraints;
- Apply an optimization method, defined above, to the model;
- Find the maximum specific power output;
- Analyze the results.

The optimization process was carried out for five types of energy conversion systems and two different cases, geothermal fluid produced from wells with no excess enthalpy and geothermal fluid produced from wells with excess enthalpy, for different geothermal fluid sources.

5.2 Design variables and constraints

The design variables and constraints for each power cycle are shown in Table 5.1. Constraints details are described as follows:

- **Dryness of turbine exhaust**
  The wellhead/separator pressure is limited by the steam quality of the turbine exhaust which should not be lower than 0.85. Otherwise, excessive droplets can cause low turbine efficiencies and power losses. The droplet formation at the last stage of the turbine can also cause severe blade erosion.
- **Lower limit of LP separator in double flash power cycle**
  This is set to be 1 bar because it is not possible to flash the excess brine from the HP separator to a vacuum pressure by a throttle valve. Also, it is not practical to operate the LP separator at a pressure below atmospheric pressure because the waste brine would have to be pumped out from the separator.
- **Lower limit of condenser pressure in ORC which is powered by spent steam**
  The condenser pressure must be set higher than the atmospheric pressure in order to handle pressure drop in the boiler. The lower limit is set to be 1.5 bar.
- **Maximum separator pressure**
  The separator pressure is related to the wellhead pressure. The wellhead pressure determines the total mass flow produced by the well. Generally, as the wellhead pressure increases, the total mass flow will decrease. A decision on the separator pressure which relates to the turbine

pressure must also take into account the pressure drop projection during long time production. Designing the separator pressure at very high values is not the best decision for the long run, because the pressure could decline over the years and, as a consequence, the wells would not be able to supply the geothermal fluid to the turbine at a high turbine pressure as it could in the early production stages. As an example, the 3x50 MW Reykjanes units 1-3 in Iceland use a turbine inlet pressure of 19 bara. The turbine type is a condensing steam turbine with condenser pressure of 0.1 bar. The 30 MW Rotokawa in New Zealand uses a separator pressure of 25.5 bara to maximize the benefits of a back-pressure turbine. The plant utilizes both exhaust steam from the back-pressure steam turbine and separated brine for a binary turbine. (Legmann, 2003) In this analysis, the upper limit for the separator pressure was set to 20 bar, based on the examples above.

TABLE 5.1: Design variables and constraints

Energy conversion system	Design variable	Constraint
Single flash system	Separator pressure	Dryness of turbine exhaust ≥ 0.85 SSI ≤ 1.2
Double flash system	HP separator pressure LP separator pressure	Dryness of HP turbine exhaust ≥ 0.85 Dryness of LP turbine exhaust ≥ 0.85 LP separator pressure ≥ 100 kpa SSI ≤ 1.2
Brine bottoming binary system	Separator pressure Boiler pressure Mass flow of ORC fluid	Dryness of steam turbine exhaust ≥ 0.85 Pinch at boiler ≥ 5°C Pinch at recuperator ≥ 5°C SSI ≤ 1.2
Spent steam bottoming binary system	Separator pressure Condenser pressure Boiler pressure Mass flow of ORC fluid	Dryness of steam turbine exhaust ≥ 0.85 Separator pressure ≤ 20 bar Pinch at boiler ≥ 5°C Condenser pressure ≥ 1.5 bar SSI ≤ 1.2
Hybrid system	Separator pressure Steam condenser pressure Boiler pressure ORC#1 Condenser pressure ORC#1 Mass flow of ORC#1 fluid Boiler pressure ORC#2 Mass flow of ORC#2 fluid	Dryness of steam turbine exhaust ≥ 0.85 Separator pressure ≤ 20 bars Pinch at boiler ORC#1 ≥ 5°C Condenser pressure ORC#1 ≥ 1.5 bar Pinch at boiler ORC#2 ≥ 5°C Pinch at recuperator ORC#2 ≥ 5°C SSI ≤ 1.2

- **Pinch in heat exchanger**
  The pinch is a minimum temperature difference between hot and cold fluid in a heat exchanger (boiler, recuperator and condenser). Lowering the pinch will increase the effectiveness of the heat exchanger and, therefore, in the case of a binary cycle, the power produced by the turbine will also increase. But it has to be considered that decreasing the pinch has the consequence of rapidly increasing the required heat exchanger area. Therefore, for economical reasons, the minimum pinch value (boiler, recuperator and condenser) was selected as 5°C, which is a common design value.

The following general assumptions are made in this analysis:

- **Isentropic efficiency**
  The isentropic efficiency assumption for pumps and compressors is 70%. Dry turbine efficiency, η_{td} is assumed to be 85%. For wet expansion in single and double flash units, the turbine efficiency is corrected by using the Baumann rule.

- **Condenser pressure**
  The lower limit for the condenser is based on the assumption that cooling water enters the condenser at 30°C. By applying 10°C for increased temperature and 5°C pinch in the condenser, the condensing temperature is at 45°C. By referring to that temperature, the low pressure limit for a condenser in the flashing system is 0.1 bar and for a binary system with n-pentane as the working fluid, the low condenser pressure limit is 1.36 bar, based on the temperature limit.
- **Non Condensable Gases (NCG)**
  The quantity of NCG in the geothermal fluid is assumed to be 0.5% by weight of fluid from the wells. NCG will be extracted from the condenser by using a compressor.
- **Overall heat transfer coefficient**
  The overall heat transfer coefficients (U) are used to calculate the area required for the heat exchanger. They are assumed to be as shown in Table 5.2 (Holman, 2002 and Engineering toolbox, 2010).

TABLE 5.2: The overall heat transfer coefficient of the heat exchanger

Fluid	**Overall heat transfer coefficient (W/m^2K)**
Water – Water	2000
Steam – Water	2000
Water – Pentane	1200
Steam – Pentane	1200
Pentane – Pentane	1200

6. RESULTS AND DISCUSSION

Two different cases are considered due to variability of wells discharge enthalpy with reservoir temperature

a. No excess enthalpy wells

In this case the geothermal fluid is produced from wells with no excess enthalpy. The discharge enthalpy of the wells is the same as the enthalpy of saturated liquid at the reservoir temperature. The range of resource temperature to be optimized is from 200 to 300°C which corresponds to a fluid enthalpy of 852 to 1345 kJ/kg. Here, the phase of the geothermal fluid at a given separator pressure is two-phase (water dominated).

Optimization in each power cycle system will be conducted for two cases:

- Silica scaling is ignored (theoretic)
- Silica scaling is taken into account (actual)

This was done to clarify the effect of resource temperatures on the optimum specific power output and optimum design parameters.

b. Excess enthalpy wells

In this case, the geothermal fluid is produced from wells with excess enthalpy. The discharge enthalpy of the wells is higher than the enthalpy of saturated liquid at the reservoir temperature. The range of reservoir temperature to be optimized is from 240 to 300°C and the range of fluid enthalpy is from 1400 to 2200 kJ/kg. Here, the phase of geothermal fluid at separator pressure is a two-phase condition with varying dryness depending on the enthalpy.

6.1 Optimization of a single flash system

The present section is an optimization analysis of a single flash system. The silica potential at the separator brine outlet and the steam quality of the turbine exhaust are the main constraints in a single flash system optimization process.

The steam quality at the turbine outlet is a constraint which limits the upper separator pressure. The steam quality of the turbine outlet decreases inversely proportionally to the separator pressure as shown in Figure 6.1. If the condenser pressure is 0.1 bar, a separator pressure of 11 bar results in 0.85 of steam quality at the turbine outlet (no interstage drainage for moisture removal). The steam quality should be maintained above 0.85 to avoid any damage to turbine blades during operation. At lower values, the droplets that are formed during the expansion process in the turbine may cause severe erosion in the last stages of the turbine blades. One possibility to increase the separator pressure limit is increasing the condenser pressure but that would reduce power output.

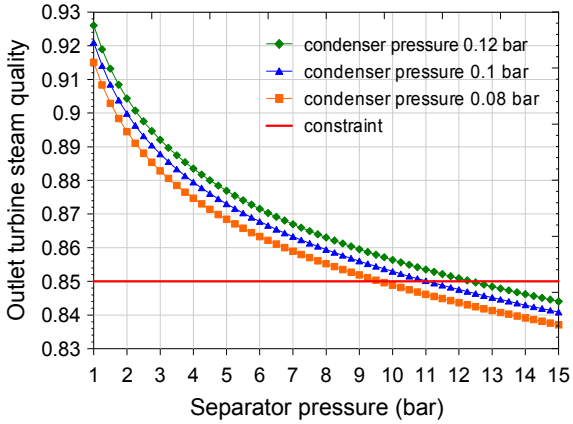

FIGURE 6.1: Steam quality at turbine outlet as a function of separator pressure

The silica scaling potential is a constraint that limits the lower separator pressure. Figure 6.2 shows the minimum flashing pressure as a function of the reservoir temperature. The minimum flashing pressure increases proportionally to the reservoir temperature. Special attention should be given to the silica scaling problem if the flashing process is performed at a lower pressure than the minimum limit.

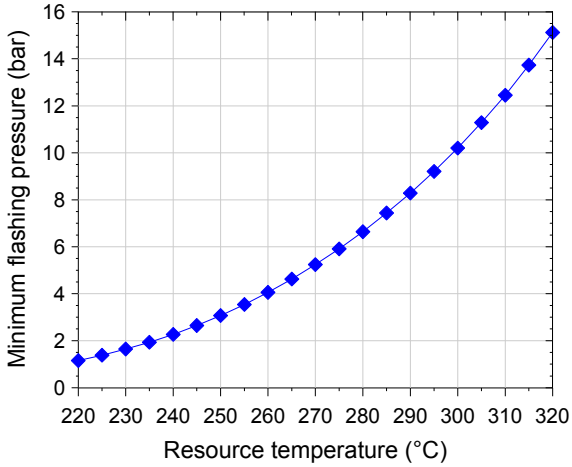

FIGURE 6.2: Minimum flashing pressure as a function of reservoir temperature

Case A (no excess enthalpy wells)

In single flash systems, the optimum specific power output for different resource temperatures is shown in Figure 6.3. The specific power output increases from 55.1 to 153.6 kW/(kg/s) as the resource temperature increases from 200 to 300°C. The silica scaling potential, which can be predicted from the resource temperature, has a small effect on the optimum power output as shown in Figure 6.3. For a resource temperature of 300°C, the difference in the optimum power output is less than 1%. The silica scaling potential has a significant effect on the optimum separator pressure for a resource temperature over 260°C, as shown in Figure 6.4. In order to prevent the deposition of silica on the brine, for resource temperatures above 260°C, the setting for the separator pressure is higher than the optimum separator pressure without silica constraint.

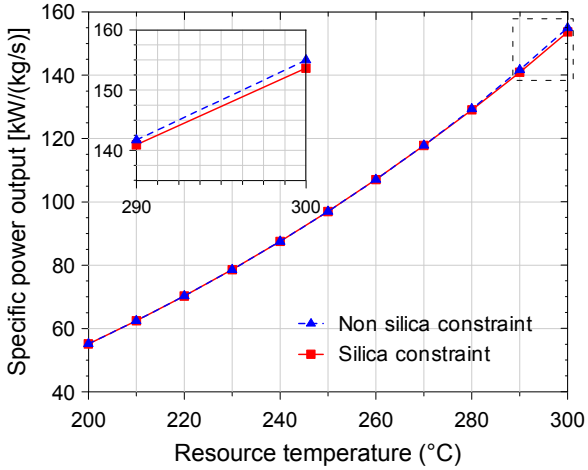

FIGURE 6.3: Optimized specific power output of a single flash system

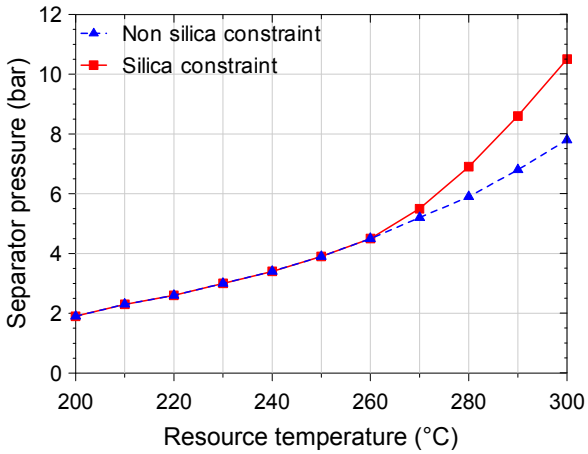

FIGURE 6.4: Optimized separator pressure of a single flash system

Case B (excess enthalpy wells)

Figure 6.5 shows the optimized specific net power output as a function of fluid enthalpy in a single flash system for the case of excess enthalpy.

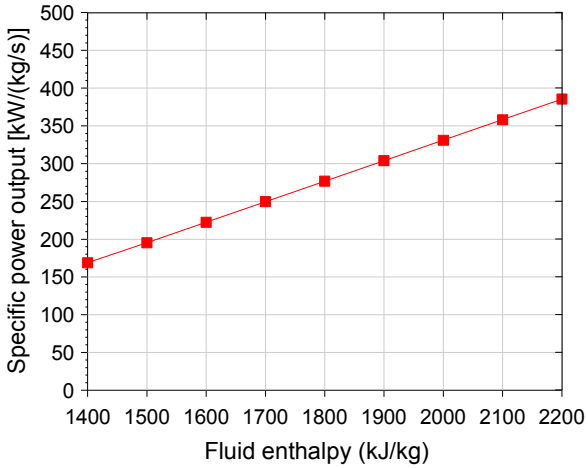

FIGURE 6.5: Optimized specific power output of a single flash system as a function of fluid enthalpy

As shown in Figure 6.5, the optimum net power output increases from 168.8 to 358.4 kW/(kg/s) as the fluid enthalpy increases from 1400 to 2200 kJ/kg.

For a single flash system, the effect of the separator pressure on specific power output for different fluid enthalpies is shown in Figure 6.6, where the optimum separator pressure increases proportionally to the enthalpy.

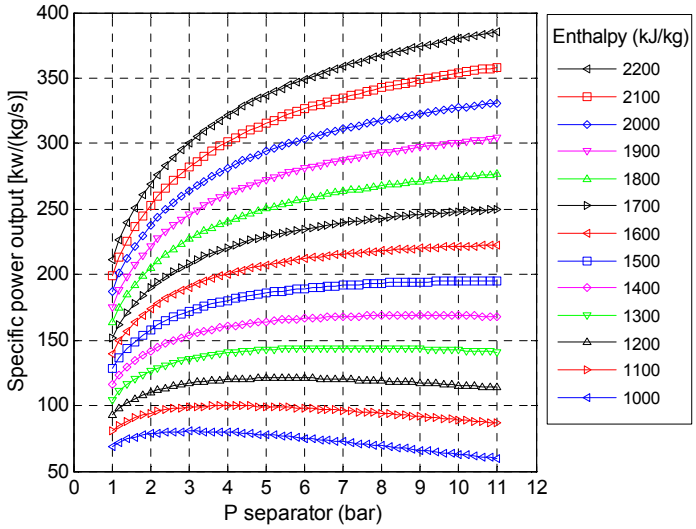

FIGURE 6.6: Specific net power output of a single flash system as a function of separator pressure and fluid enthalpy

The optimum separator pressure of a single flash system as a function of fluid enthalpy is shown in Figure 6.7. For fluid enthalpy of 1500 kJ/kg and higher, the optimum separator pressure remains constant at 11 bar due to the restriction of steam quality at the turbine outlet.

Figure 6.8 shows that for fluid enthalpy from 1400 to 1500 kJ/kg, the exhaust steam quality decreases sharply to 0.85. For separator pressures higher than 11 bar, there is a potential problem related to the droplets formed in the turbine.

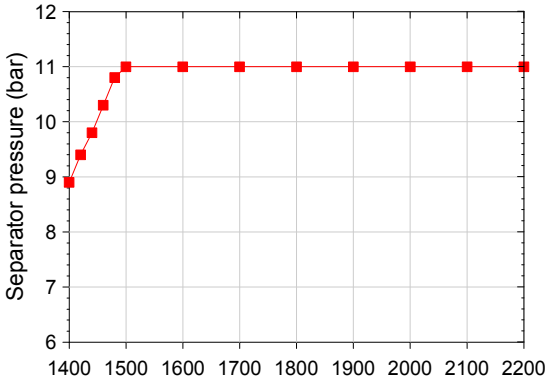

FIGURE 6.7: Optimized separator pressure of a single flash system as a function of fluid enthalpy

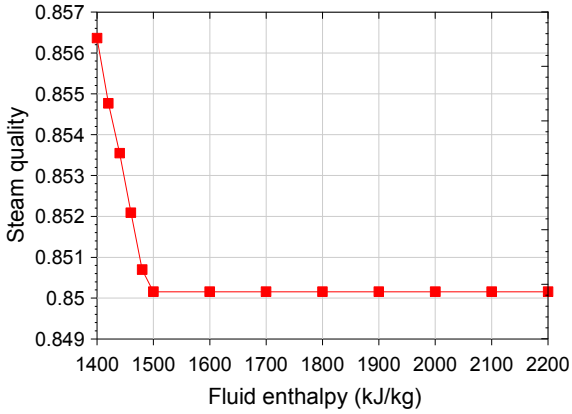

FIGURE 6.8: Steam quality at turbine outlet of a single flash system as a function of fluid enthalpy

All the figures are similar for all reservoir temperatures. Silica scaling potential does not affect the optimum separator pressure value because the optimum separator pressure value is always higher than the lower separator pressure limit.

6.2 Optimization of double flash system

Case A (no excess enthalpy wells)

Figure 6.9 shows the optimized specific power output from high and low pressure turbines assuming different silica constraints. In low pressure turbines, the steam exhaust goes through the condenser at vacuum pressure levels. This is the main factor of the high power output in the low pressure turbine. A dashed line in Figure 6.9 b represents the specific power output from the single flash system. For temperature resources lower than 300°C, the double flash system gives higher specific power than the single flash system.

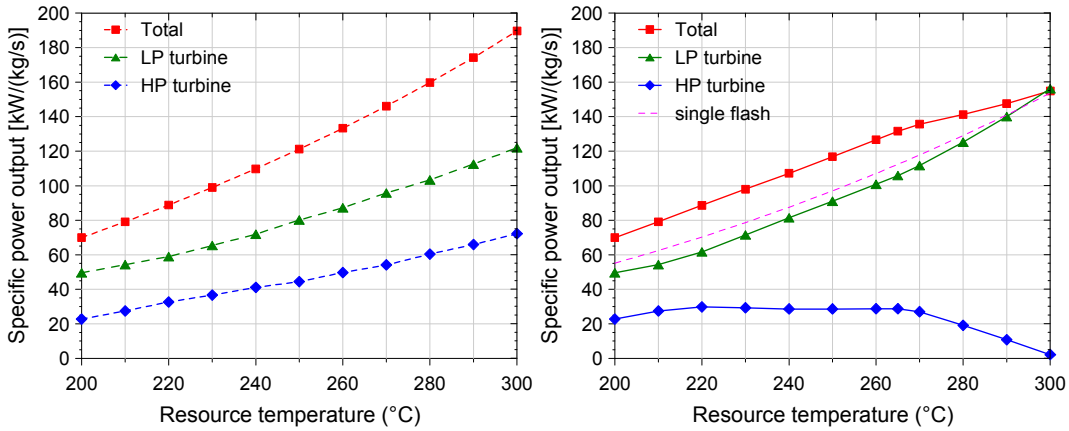

FIGURE 6.9: Optimized specific power output of individual turbines in a double flash system

Figure 6.10 shows the corresponding separator pressure for the optimum specific power output assuming different silica constraints. Optimum pressure for a low pressure separator increases proportionally to the resource temperature to prevent silica deposition in the brine. The optimum setting value for the HP separator pressure becomes higher when the resource temperature increases from 200 to 265°C. It decreases for resource temperatures between 265 and 300°C due to the restriction of the steam quality at the LP turbine outlet as shown in Figure 6.11. At 300°C, the gap between the optimum pressure of the high pressure and the low pressure separators is small as shown in Figure 6.10(b). Therefore, the power output from high pressure turbine is not significant.

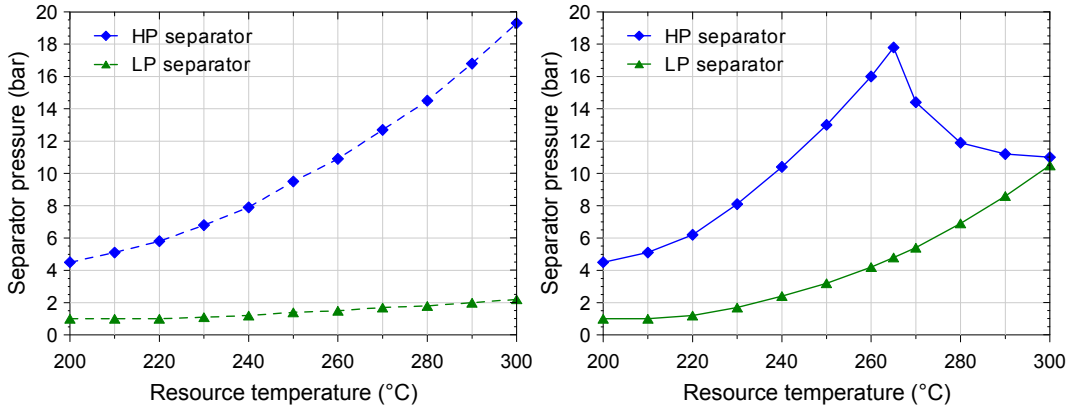

FIGURE 6.10: Optimized separator pressure of a double flash system

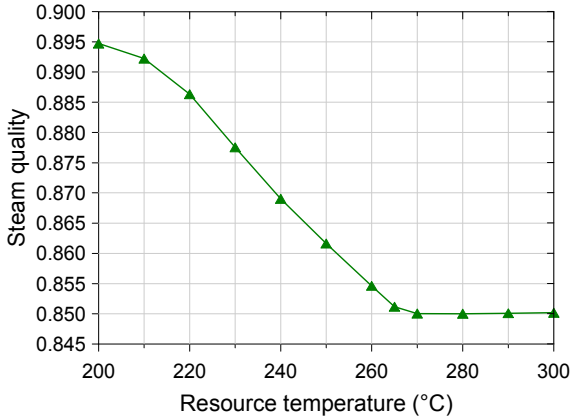

FIGURE 6.11: Steam quality at LP turbine exhaust of a double flash system

If the optimization process is carried out without regard to silica scaling, the Silica Saturation Index (SSI) will increase directly proportional to the resource temperature as shown in Figure 6.12. The SSI increases from 0.95 to 2.39 for resource temperatures between 200°C and 300°C.

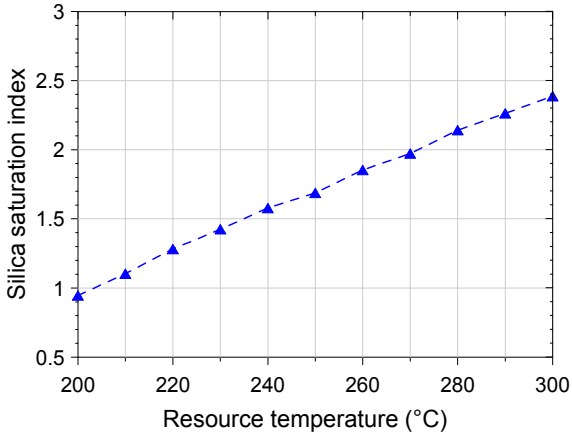

FIGURE 6.12: SSI in the excess brine of a double flash system

Figure 6.13 shows the reinjection temperature at optimum condition of a double flash system. The difference between those two graphs indicates the effect of silica scaling. The optimized specific power output of a double flash system for different silica constraints is shown in Figure 6.14.

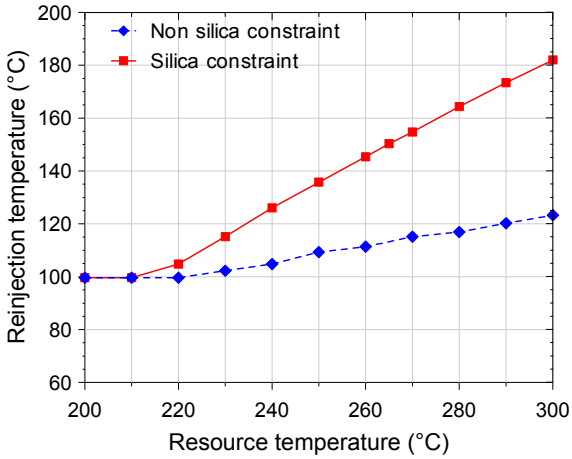

FIGURE 6.13: Optimized reinjection temperature and optimized specific power output of a double flash system

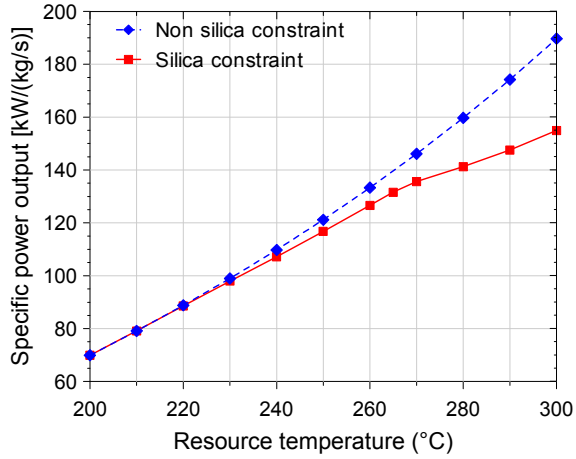

FIGURE 6.14: Optimized reinjection temperature and optimized specific power output of a double flash system

Case B (excess enthalpy wells)

The optimized specific power output from high and low pressure turbines as a function of fluid enthalpy for different reservoir temperatures is shown in Figure 6.15. Power output from the LP turbine dominates the total power output. The LP turbine contributed power output increases proportionally to the resource temperature, because there is a higher LP separator pressure limit for the hotter temperature resources due to the silica scaling potential.

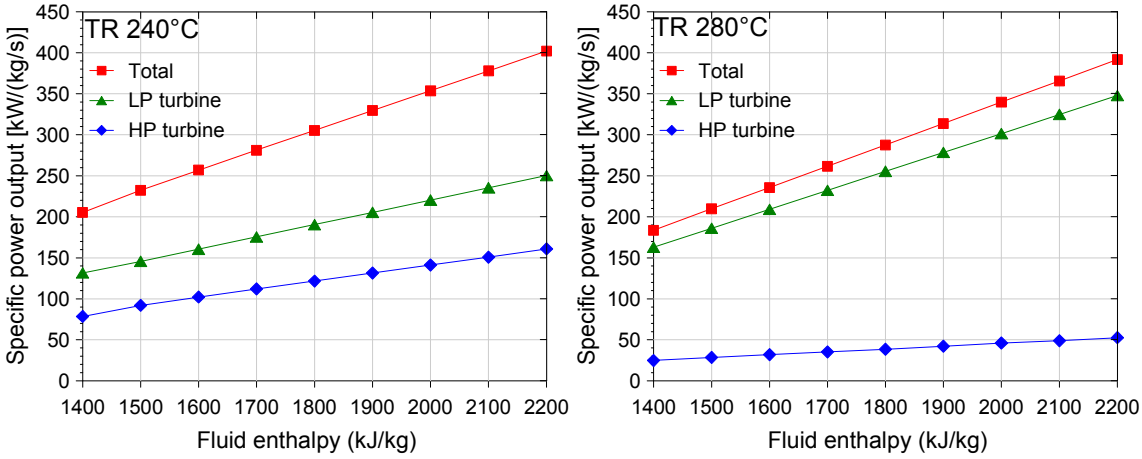

FIGURE 6.15: Optimized specific power output of HP and LP turbines in a double flash system

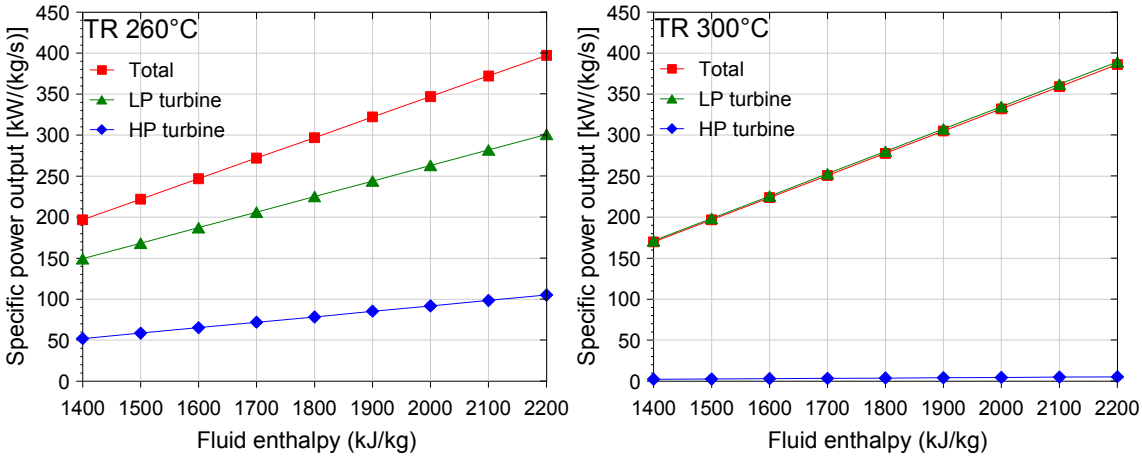

FIGURE 6.15: Continued - optimized specific power output of HP and LP turbines in a double flash system

The optimum separator pressure for these cases is shown in Figure 6.16. The optimum pressure of the HP separator is lower at a higher resource temperature to prevent steam quality of below 0.85 of the LP turbine exhaust. The margin between the optimized pressure of HP and LP separators in hotter resource temperature is smaller, therefore the power output of the HP turbine is also smaller.

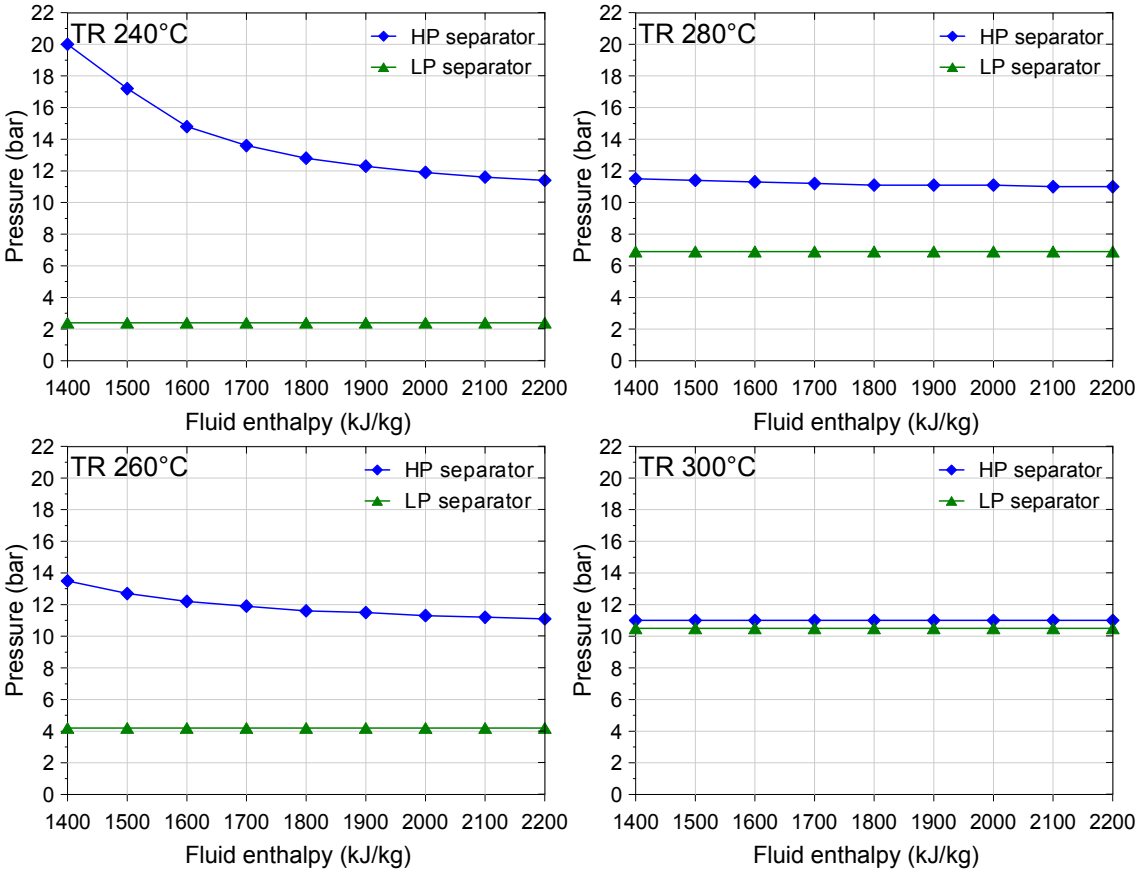

FIGURE 6.16: Optimized HP and LP separator pressure for different reservoir temperatures in a double flash system

Figure 6.17 shows a contour graph of the specific power output with 1500 kJ/kg fluid enthalpy in a double flash system. Based on the graph, it is possible to determine if the separation pressure is set to the optimum value. The square black dot shows the optimum variable and the contour values show the ratio of the optimum specific power output. The pressure ratio in the y-axis of the graph is defined as:

$$\text{Pressure ratio} = \frac{p_{LP} - p_C}{p_{HP} - p_C}$$

where, p_{LP} is the low separation pressure, p_{HP} is the high separation pressure and p_c is the condenser pressure.

The area located outside the contours represents an illegal solution (constraint violation). The lower left of the contour is restricted by the silica scaling potential and the upper right is restricted by the steam quality of the LP turbine exhaust. In a high-temperature resource, the selection of the operational parameter (HP and LP separator pressure) is very limited.

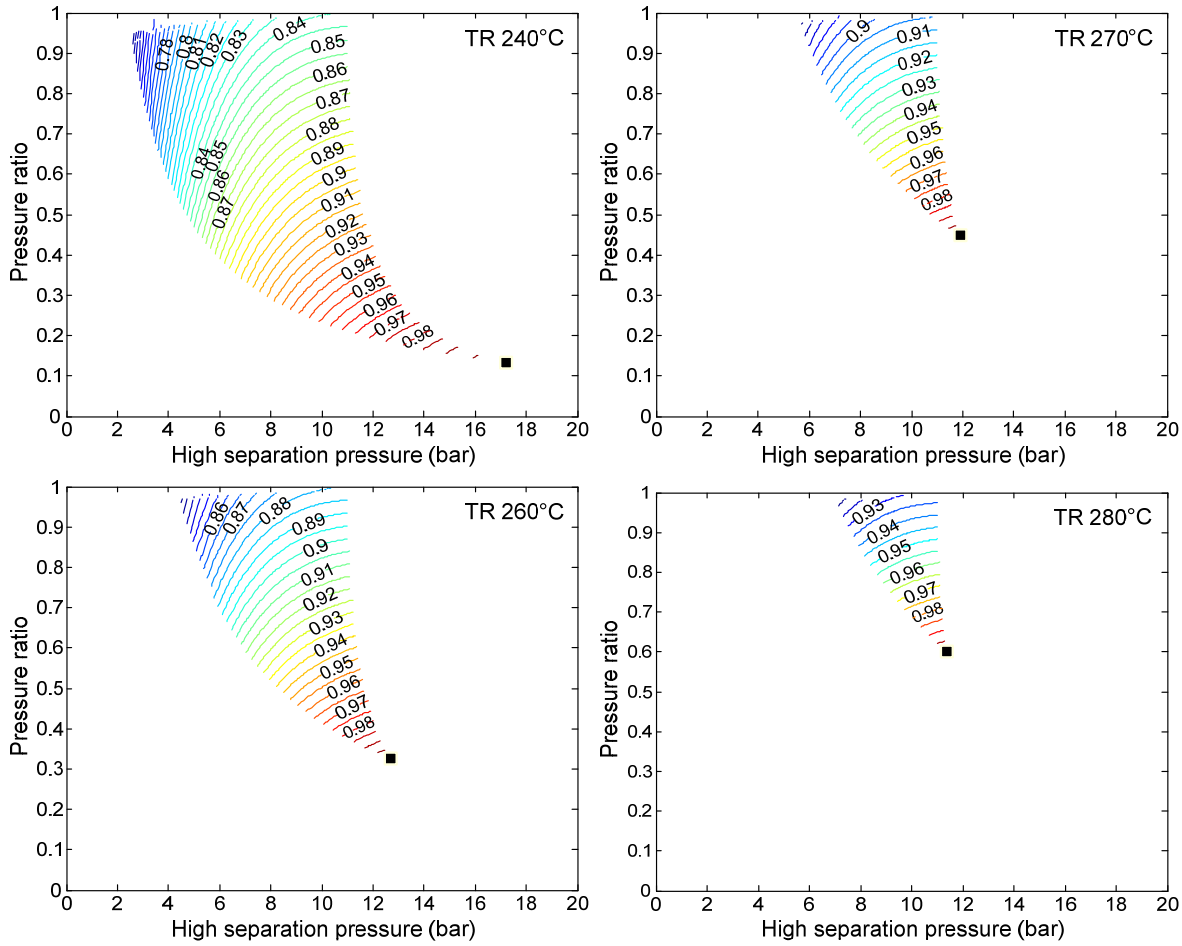

FIGURE 6.17: Specific power output ratio as a function of a HP separator in a double flash system

The optimized power output when utilizing geothermal fluid from different reservoir temperatures using double flash systems is shown in Figure 6.18. The specific power output produced from hotter reservoir temperatures is lower due to the silica scaling constraint. For example, the maximum specific power output produced from geothermal fluid which has an enthalpy of 1800 kJ/kg at a resource temperature of 300°C is 278 kW/(kg/s), which is 9% smaller than for the same fluid at a resource temperature of 240°C (305.4 kW/(kg/s)). A blue dashed line (Fig. 6.18) shows the specific power output from the single flash system. For 300°C resource temperature, the double flash system gives similar power output as the single flash system.

The most common power cycle configuration in utilizing geothermal fluid from high-temperature fields is a single flash condensing system. One of the reasons is that it has low risk for silica scaling. Compared to other configurations (double flash and brine bottoming binary system), a single flash cycle with a condensing turbine has the lowest power output production. Figure 6.19 shows the percentage of additional specific power output for different temperature reservoirs using double flash systems, using the single flash system as a reference. The percentage of additional specific power

output from hotter reservoir temperatures is smaller due to the silica scaling constraint. For example, if the origin of geothermal fluid has a resource temperature of 240°C, the power output from a double flash system utilizing a fluid enthalpy of 1800 kJ/kg is 10.3% higher than for the single flash system, but if the resource temperature is at 300°C, the additional power is only 0.4%.

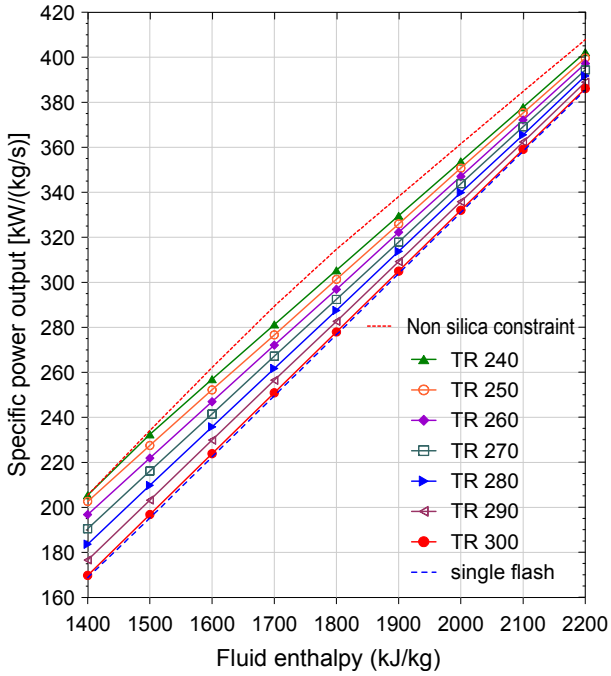

FIGURE 6.18: Optimized specific power output
for different reservoir temperatures in a double flash system

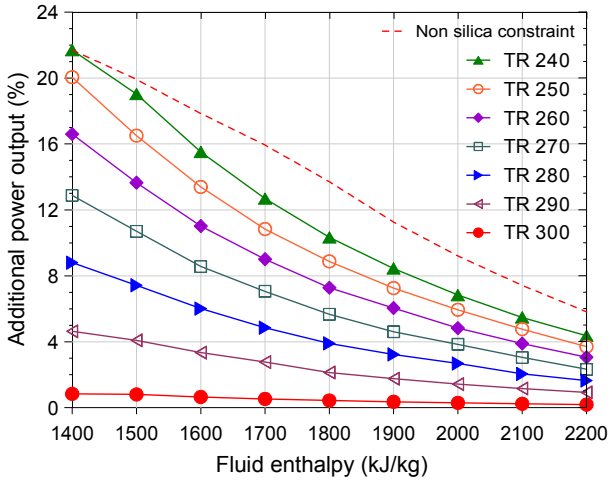

FIGURE 6.19: Percentage of additional specific power output
for different reservoir temperatures in a double flash system

6.3 Optimization of a brine bottoming binary (BBB) system

Working fluid selection

For this case of analysis, a brine bottoming binary (BBB) system consists of a single flash condensing unit and an ORC unit. Results from a thermodynamic optimization of the BBB system utilizing excess brine for a bottoming binary cycle (ORC) for different types of working fluid is shown in Figure 6.20. The highest specific total power output for a resource temperature below 210°C is obtained when isobutane is used as a working fluid.

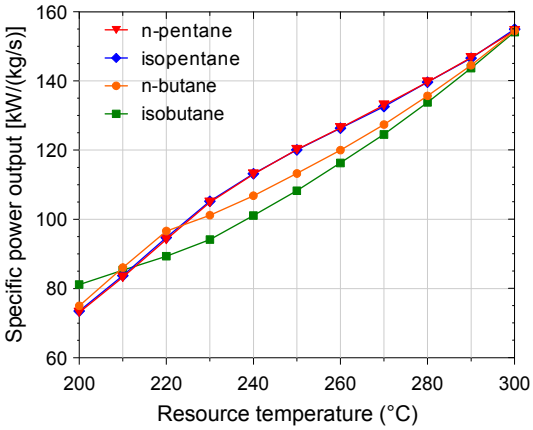

FIGURE 6.20: Optimized specific power output for different working fluids in a BBB system

Using n-pentane as a working fluid gives slightly higher specific total power output compared to isopentane, in the range of resource temperatures between 230 and 300°C. At that temperature range, the turbine power output for the case of isopentane is slightly higher compared to n-pentane. But due to a higher requirement for parasitic load (power demand of the pumps and cooling tower fans), the net power output using isopentane is slightly lower than n-pentane. Higher power required by the pump is due to a higher requirement of optimum boiler pressure and mass flow rate of the working fluid. Table 6.1 shows the comparison of those four working fluids at a resource temperature of 250°C.

TABLE 6.1: Comparison of optimum parameters and power output for different working fluids of a BBB system at a resource temperature of 250°C

Fluid	p_{boiler} (bar)	$\dot{m}_{wf}$ (kg/s)	$\dot{W}_{turbine,ORC}$ (kW/(kg/s))	$\dot{W}_{parasitic,ORC}$ (kW/(kg/s))	$\dot{W}_{net,ORC}$ (kW/(kg/s))	$\dot{W}_{net,steam}$ (kW/(kg/s))	$\dot{W}_{total}$ (kW/(kg/s))
Isobutane	31.8	0.73	29.63	4.14	25.49	84.62	108.26
N-butane	32.9	0.53	34.36	3.90	30.46	84.62	113.23
Isopentane	18.8	0.65	39.50	2.22	37.29	84.62	120.05
N-pentane	15.7	0.49	39.09	1.74	37.35	84.62	120.11

Due to the highest specific total power output in most of the resource temperature range, n-pentane is selected as a working fluid for the BBB system.

Case A (no excess enthalpy wells)

In the no-excess enthalpy wells case, the optimum specific power output of a brine bottoming binary (BBB) system is estimated for different resource temperatures. The optimized specific power output from different turbine types and diverse silica constraints is shown in Figure 6.21. For a resource temperature between 200 and 300°C, a BBB system gives higher specific power than a single flash system.

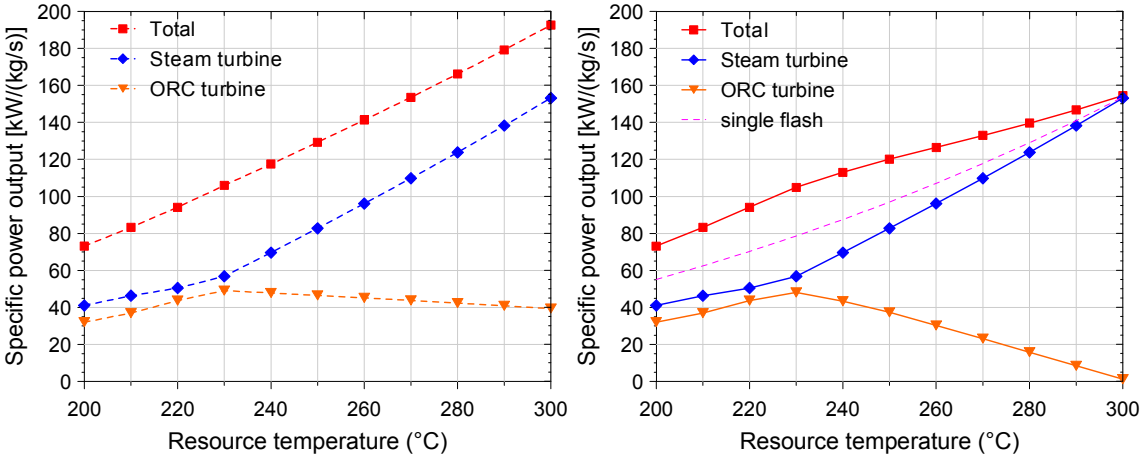

(a) non silica constraint *(b) silica constraint*

FIGURE 6.21: Optimized specific power output of an individual turbine from a BBB system

Figure 6.22 shows that the optimum separator pressure increases to a constant value (11 bar) for resource temperatures above 230°C. This behaviour is related to the steam exhaust turbine constraint as shown in Figure 6.23.

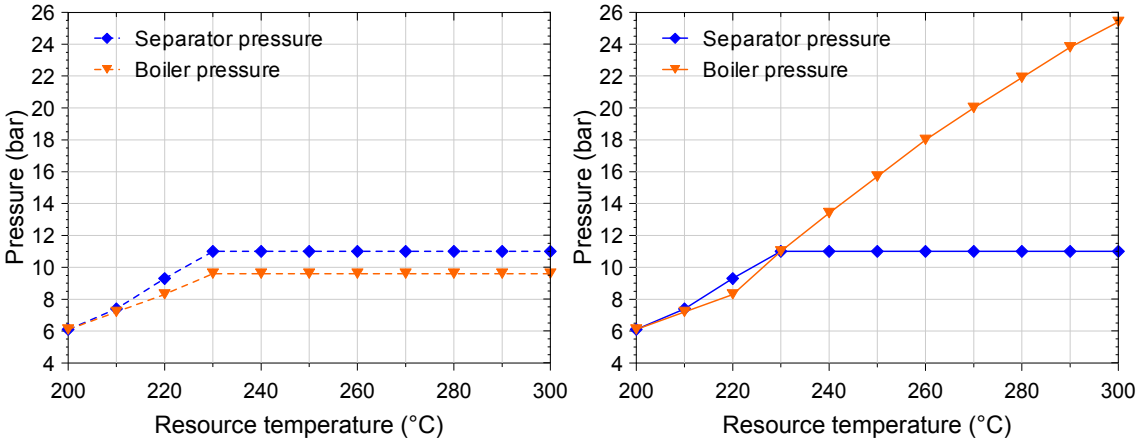

(a) non silica constraint *(b) silica constraint*

FIGURE 6.22: Optimized separator and boiler pressure of a BBB system

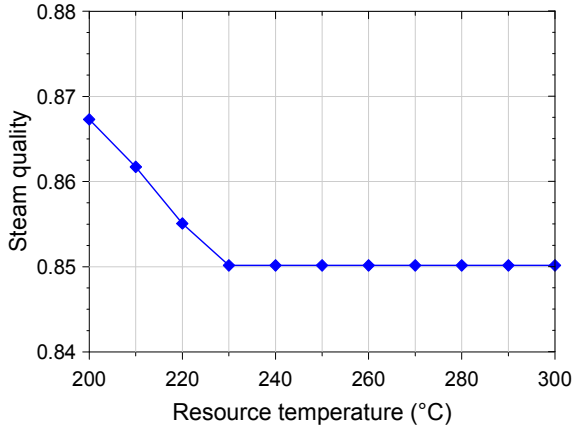

FIGURE 6.23: Steam quality of steam turbine exhaust of a BBB system

The heat-exchange diagram for the ORC boiler unit is shown in Figure 6.24, where the outlet temperature of the brine in the boiler increases proportionally to the resource temperature in order to prevent silica deposition. The optimum boiler pressure increases to maintain a minimum temperature difference between the hot brine and the cold binary fluid in the boiler.

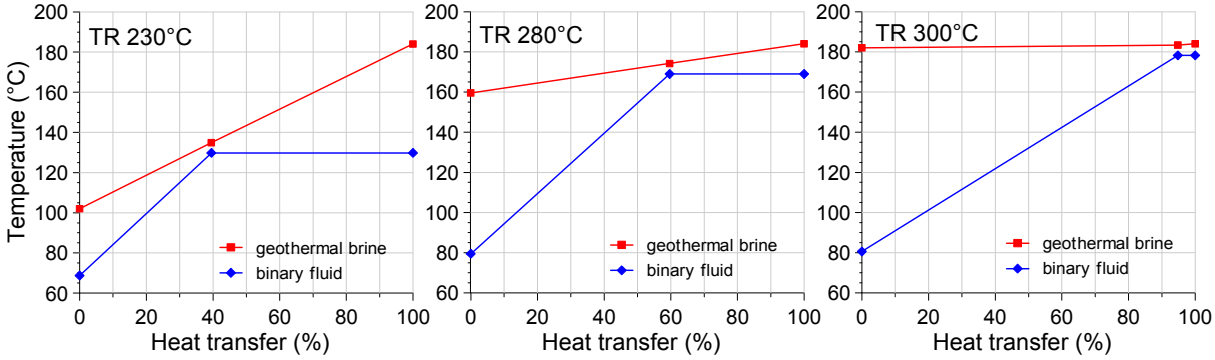

FIGURE 6.24: Temperature – heat exchange diagram of the ORC boiler at different resource temperatures. The pinch is 5°C

For a high resource temperature, a small percentage of the heat from the brine is used to evaporate the binary fluid, resulting in a small mass flow for the ORC turbine. If the separator pressure is restricted,

the brine mass flow to the boiler decreases for higher resource temperatures. In this case, less power output is obtained from the ORC unit.

If the optimization process is carried out without the silica constraint, the Silica Saturation Index (SSI) increases proportionally to the resource temperature as shown in Figure 6.25.

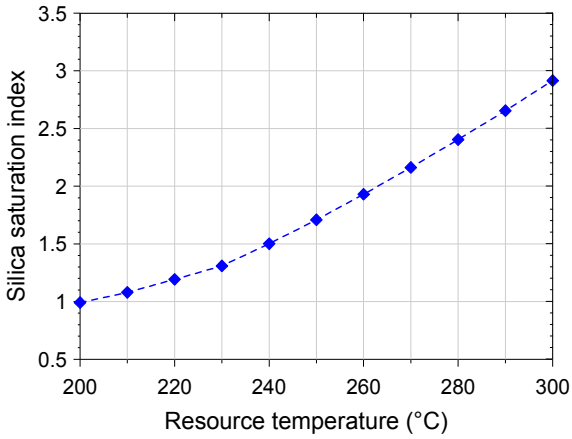

FIGURE 6.25: SSI in the excess brine of a BBB system

Figure 6.26 shows the reinjection temperature at optimum condition of a BBB system. The optimized reinjection temperature increases proportionally to the resource temperature due to silica constraint. The optimum power output of a BBB system for a resource temperature above 240°C is smaller than the power output without the silica constraint as shown in Figure 6.27

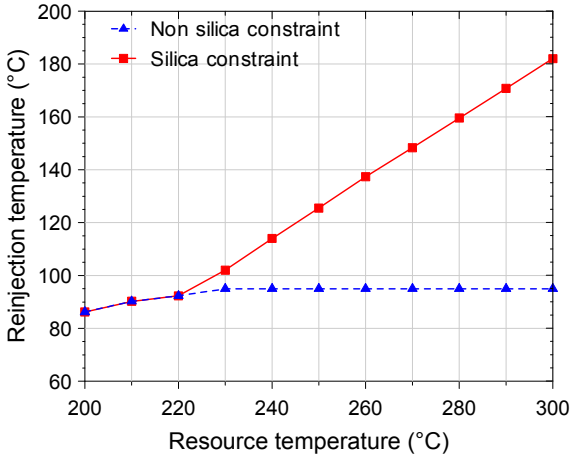

FIGURE 6.26: Optimized reinjection temperature of a BBB system

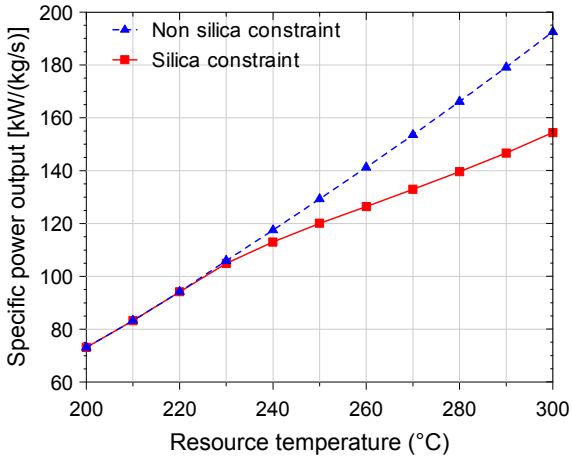

FIGURE 6.27: Optimized specific power output of a BBB system

Case B (excess enthalpy wells)

The optimized specific total power output and specific power output from the individual turbines is shown in Figure 6.28 as a function of fluid enthalpy for different reservoir temperatures in the brine bottoming binary (BBB) system. The power output of a steam turbine dominates the total power output. The power output of an ORC turbine decreases as the fluid enthalpy of the geothermal fluid increases due to less mass flow of hot brine used to heat the binary fluid at higher fluid enthalpy. °

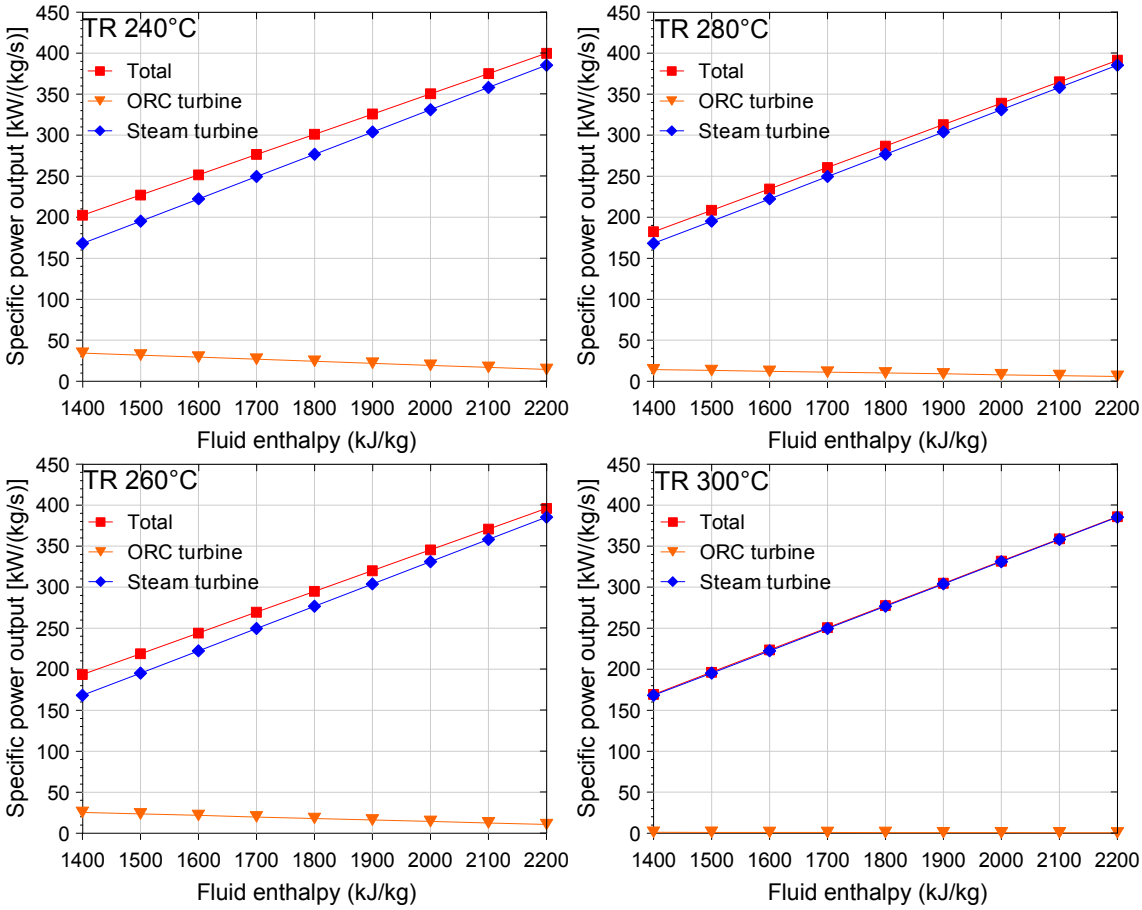

FIGURE 6.28: Optimized specific power output of individual turbines in a BBB system

The corresponding optimum pressures of the separator and the boiler are shown in Figure 6.29. The optimum pressure is a function of resource temperature and is restricted to 11 bar due to the steam turbine exhaust quality constraint. The optimum boiler pressure increases proportionally to the resource temperature in order to maintain the temperature difference between the hot brine and the cold binary fluid in the boiler.

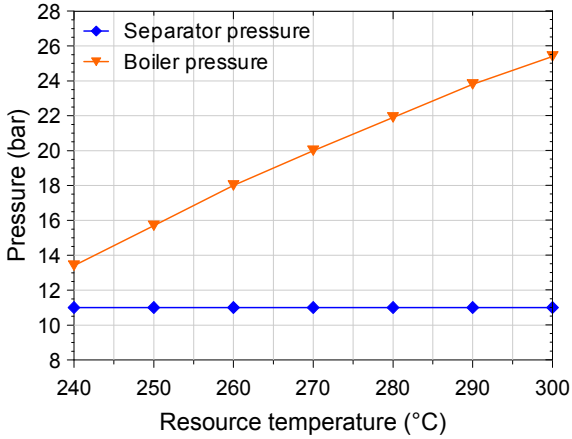

FIGURE 6.29: Optimized boiler and separator pressures for different reservoir temperatures in a BBB system

The optimized power output for different reservoir temperatures using a BBB system is shown in Figure 6.30. The specific power output from a high-temperature reservoir temperature is lower due to the silica scaling constraint. For example, the maximum specific power output produced from fluid with an enthalpy of 1800 kJ/kg for a 300°C resource is 277.6 kW/(kg/s). This power is 7.8% lower than the power from a 240°C resource (301.1 kW/(kg/s)).

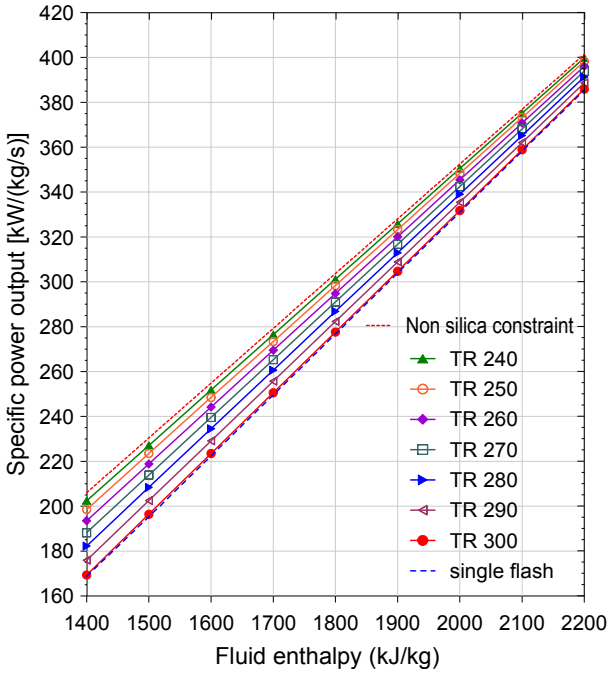

FIGURE 6.30: Optimized specific power output for different reservoir temperature in a BBB system

Figure 6.31 shows the percentage of added specific power output for different reservoir temperatures from the brine bottoming binary system, which is smaller for a high-temperature resource due to the silica scaling constraint. For a resource temperature of 240°C, the power output from a brine bottoming binary system utilizing the fluid with an enthalpy of 1800 kJ/kg is 8.8% higher than for a single flash system, but only 0.3% higher if the resource temperature is 300°C.

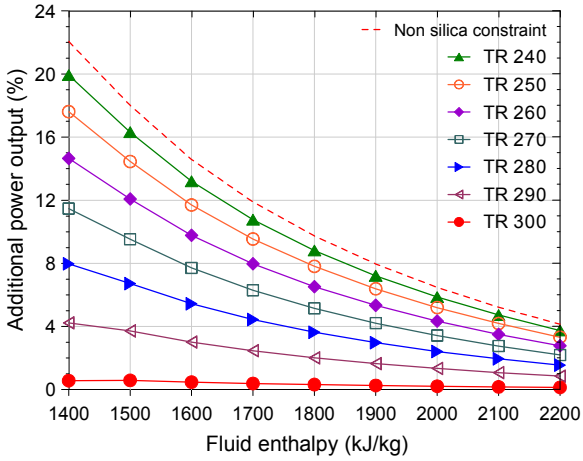

FIGURE 6.31: Percentage of additional specific power output for different reservoir temperatures in a BBB system

6.4 Optimization of spent steam bottoming binary (SSBB) system

Working fluid selection

For this case, the spent steam bottoming binary system (SSBB) consists of a single flash back-pressure unit and an ORC unit. Figure 6.32 shows the thermodynamic optimization of the spent steam

bottoming binary system using exhaust steam from a back pressure turbine. In the optimization process, various types of working fluids are used. The highest specific total power output obtained used n-pentane as working fluid, which was then selected for the SSBB system.

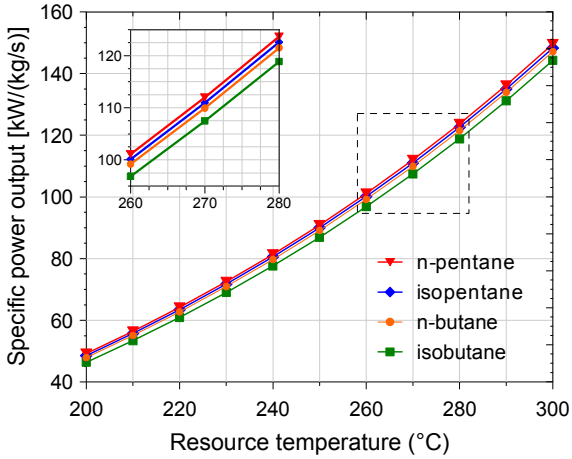

FIGURE 6.32: Optimized specific power output of different working fluids in SSBB system

Case A (no excess enthalpy wells)

The optimum specific power output of spent steam bottoming binary system (SSBB) for different resource temperatures is shown in Figure 6.33. Optimized specific power output increases from 49.2 to 149.55 kW/(kg/s) and is directly proportional to the resource temperature in the range from 200 to 300°C. The dashed line shows the single flash specific power output used for comparison with the other systems in analysis. In the present SSBB system case, the production is slightly lower than in a single flash system.

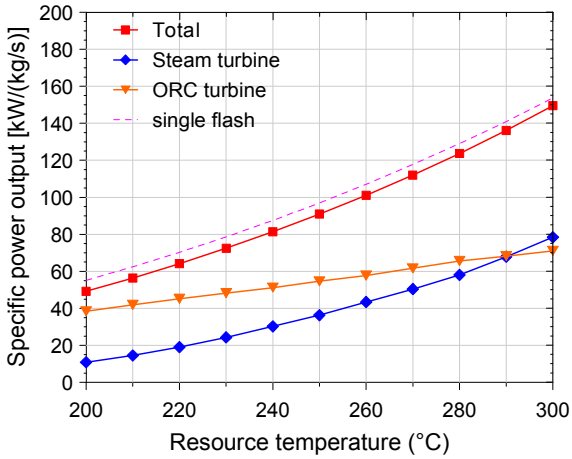

FIGURE 6.33: Optimized specific power output of individual turbines in a SSBB system

Figure 6.34 shows the corresponding pressure for the optimum specific power output. Similar to a single flash system, the optimized separator pressure increases proportionally with the resource temperature.

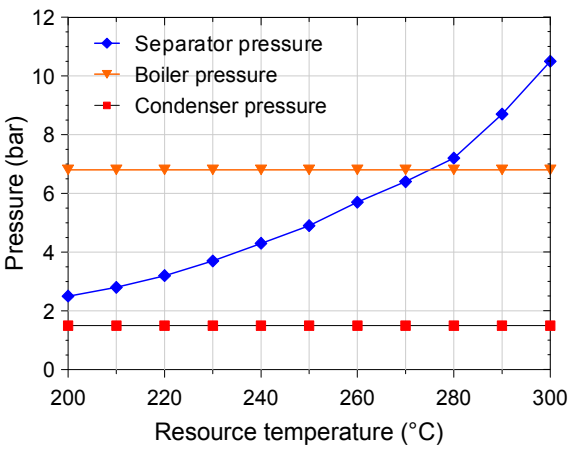

FIGURE 6.34: Optimized separator and boiler pressure in a SSBB system

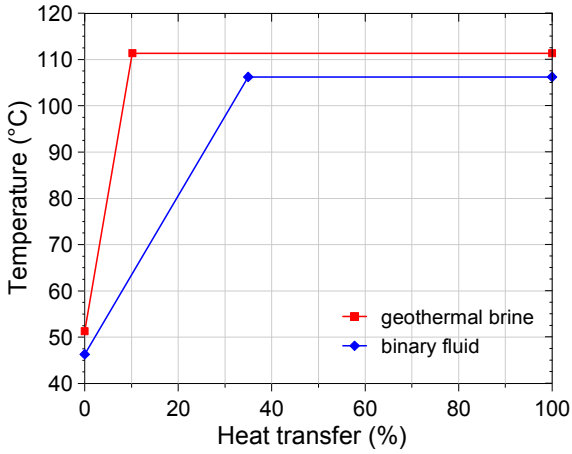

FIGURE 6.35: Temperature – heat exchange diagram of boiler from a SSBB system

Case B (excess enthalpy wells)

The optimum specific power output of spent steam bottoming binary (SSBB) system for different fluid enthalpies is shown in Figure 6.36. Optimized specific power output increases from 163.9 to 409.1 kW/(kg/s) proportionally to the fluid enthalpy. The dashed line shows the specific power output from the single flash case. In this case, a hybrid system produced slightly lower specific power than the single flash system for fluid enthalpy in the range from 1400 to 1700kJ/kg. For fluid enthalpy above 1700 kJ/kg, the system produces higher specific power output.

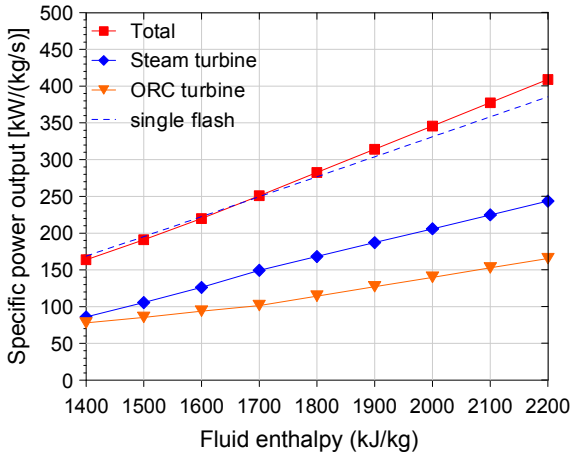

FIGURE 6.36: Optimized specific power output of individual turbines from a SSBB system

The percentage of additional specific power output from a SSBB system compared to a single flash system is shown in Figure 6.37.

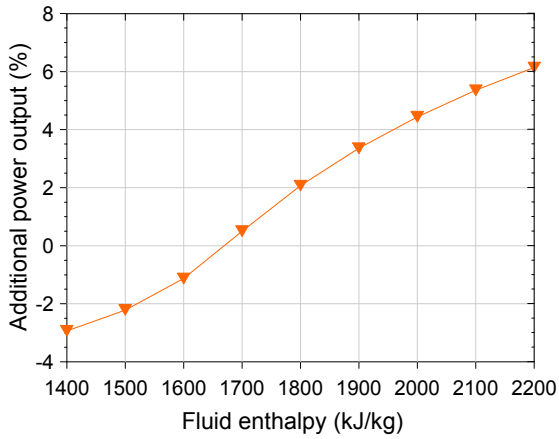

FIGURE 6.37: Percentage of additional specific power output from a SSBB system

Figure 6.38 shows the pressure for the optimum specific power output. Similar to a single flash system, the optimum separator pressure in the SSBB system increases proportionally to the resource temperature. In this case, the upper limit for the separator pressure is set to 20 bar based on the reservoir pressure restriction mentioned before. The optimized boiler pressure is constant at 680 kPa to maintain a minimum temperature difference between the hot exhaust steam from the steam turbine and the cold binary fluid in the boiler.

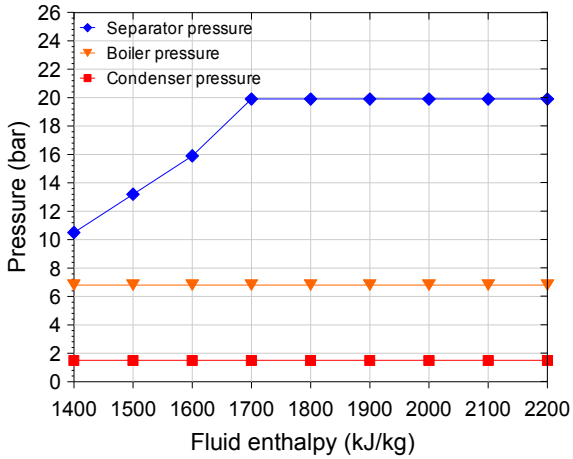

FIGURE 6.38: Optimized separator and boiler pressure of a SSBB system

The optimization result shows that the power output from the SSBB system strongly depends on the maximum design separator pressure. This correlation is shown in Figure 6.39. If the wells can supply a high separator pressure, the SSBB system produces higher specific power output than a single flash system.

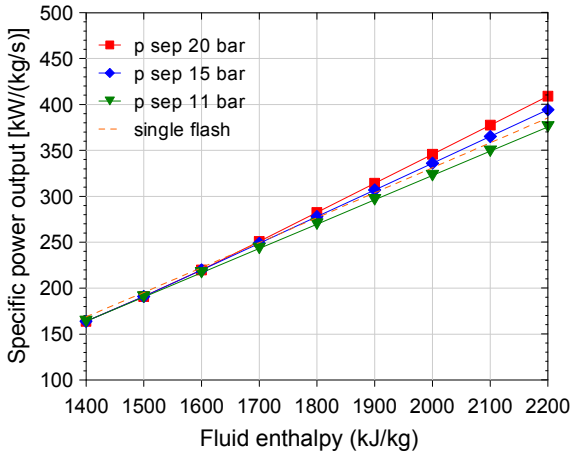

FIGURE 6.39: Specific power output of a SSBB system as a function of fluid enthalpy and maximum separator pressure

For all reservoir temperatures, the optimized power output and working pressure are similar. The silica scaling potential does not affect optimum separator pressure values because this configuration uses steam for the binary unit instead of brine, and the optimum separator pressure is higher than the lower pressure limit given in the silica constraint.

6.5 Optimization of a hybrid system

Case A (no excess enthalpy wells)

As already discussed in a previous section, n-pentane gives higher power output when it is used as the working fluid for the brine bottoming binary system and the spent steam bottoming binary system. Therefore, n-pentane was selected as a working fluid for the hybrid system.

In a hybrid system, the optimum specific power output for individual units (steam turbine, steam-powered ORC turbine, and brine-powered ORC turbine) for different resource temperatures and diverse silica constraints is shown in Figure 6.40. The optimized specific power output increases from 71.2 to 165.4 kW/(kg/s) proportionally to the resource temperature (200 to 300°C). The dashed line (Fig. 6.40 b) represents the specific power output from the single flash system. The hybrid system gives higher specific power than a single flash system for all resource temperature ranges.

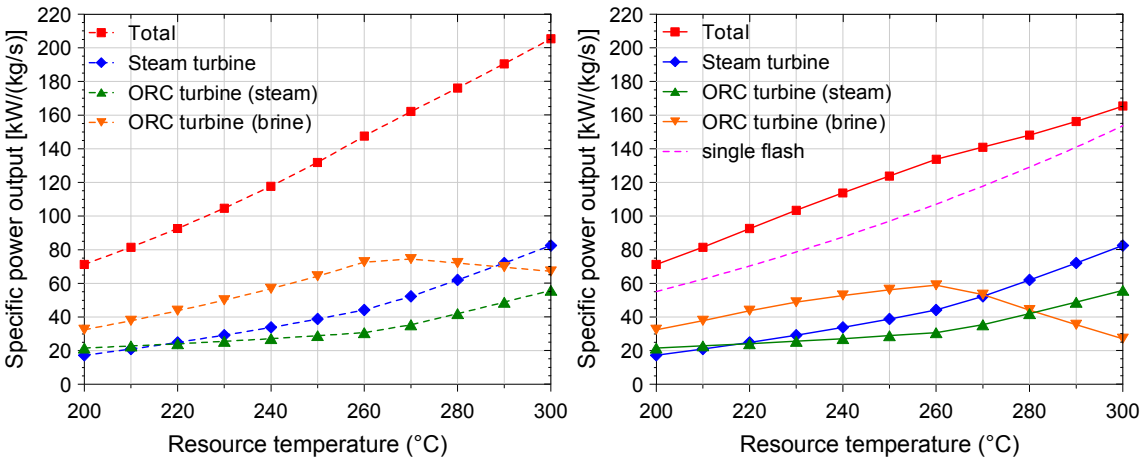

(a) non silica constraint *(b) silica constraint*

FIGURE 6.40: Optimized specific power output of individual turbines in a hybrid system

Figure 6.41 shows the corresponding pressure for the optimum specific power output. In this case, the upper limit of the separator pressure is set to 20 bar, based on the assumed maximum separator pressure. Optimum separator pressure increases proportionally to the resource temperature until the maximum pressure of 20 bar is reached. For a binary cycle where exhaust steam is used, the optimum boiler pressure is constant at 680 kPa due to constant condensation exhaust steam pressure at 150 kPa. In a binary cycle where separated brine is used, the optimum boiler pressure increases proportionally to the separator pressure to maintain minimum temperature differences in the boiler.

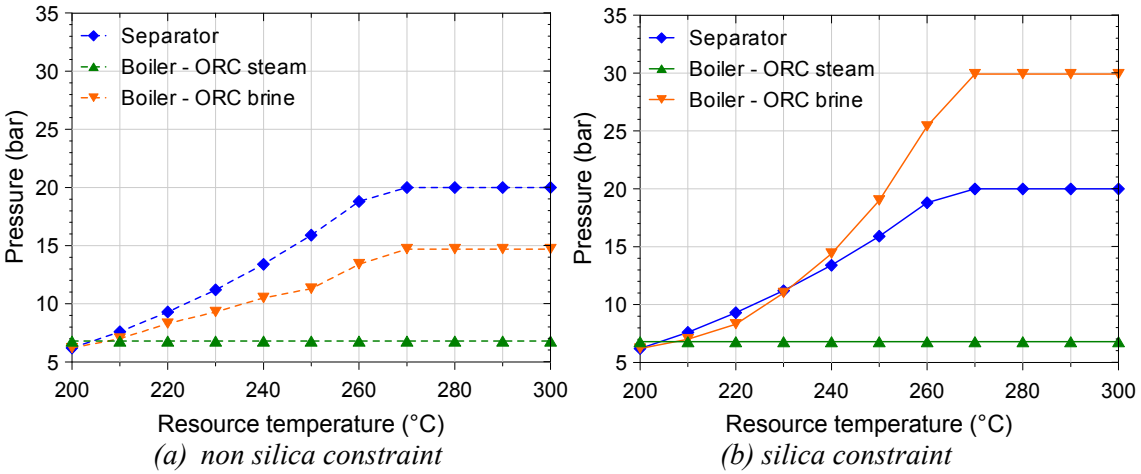

(a) non silica constraint *(b) silica constraint*

FIGURE 6.41: Optimized separator and boiler pressures of a hybrid system

If the optimization process is carried out without the silica constraint, the Silica Saturation Index (SSI) increases proportionally to the resource temperature as shown in Figure 6.42.

Figure 6.43 shows the reinjection temperature at optimum condition of a hybrid system for different silica constraints. The optimized reinjection temperature increases proportionally to the resource temperature due to silica constraint. The optimum specific output power with silica constraint at resource temperatures above 240° C is smaller than the non silica constraint as shown in Figure 6.44.

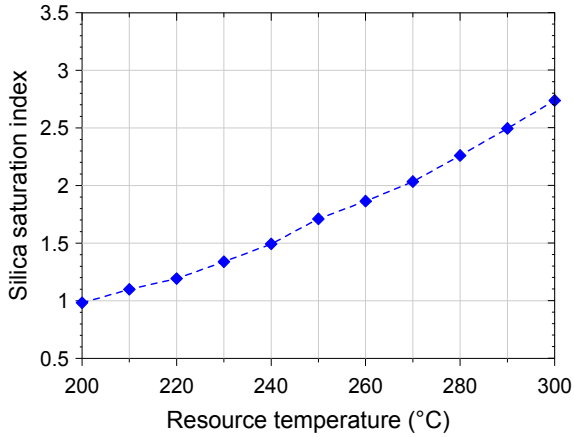

FIGURE 6.42: SSI in the excess brine of a hybrid system

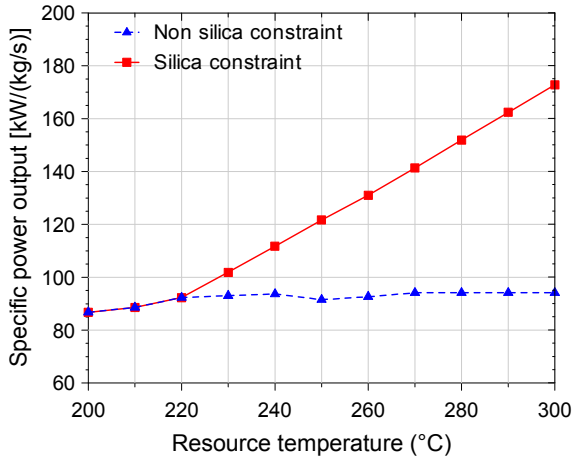

FIGURE 6.43: Optimized reinjection temperature of a hybrid system

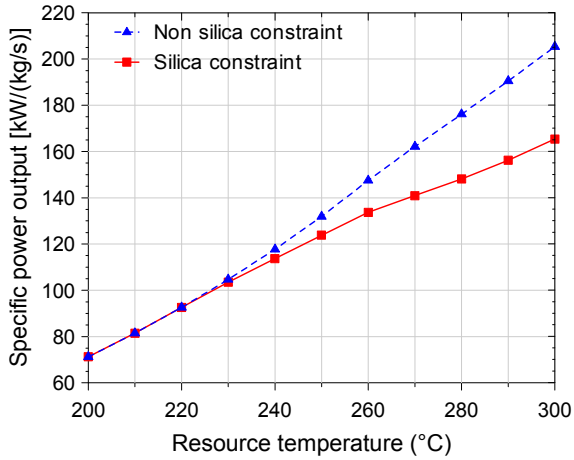

FIGURE 6.44: Optimized specific power output of a hybrid system

Case B (excess enthalpy wells)

The optimized specific power output for each unit and the total power output in a hybrid system are shown in Figure 6.45. The total specific power output has a major contribution from the back-pressure steam turbine. Power output from the brine-powered ORC turbine decreases inversely proportionally to the fluid enthalpy due to the lower mass flow of brine to heat the working fluid.

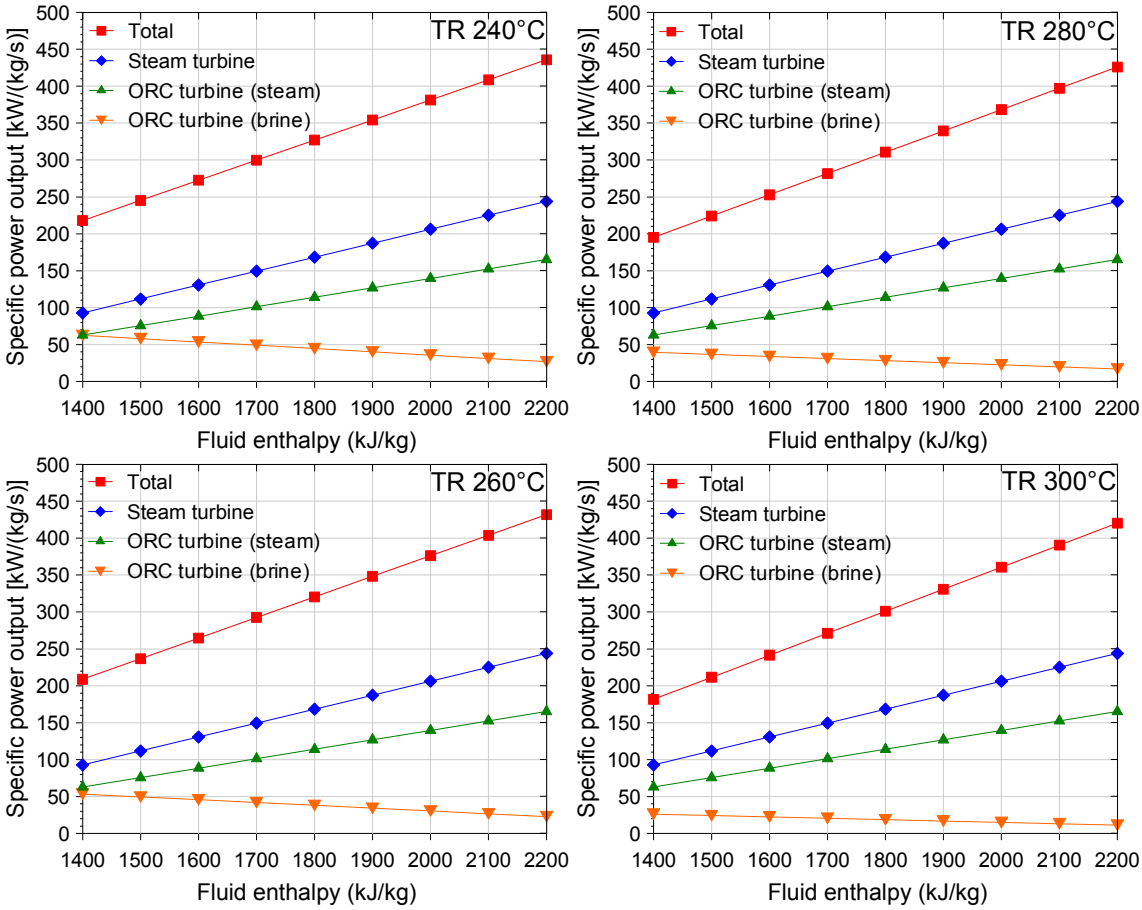

FIGURE 6.45: Optimized specific power output of individual turbines in a hybrid system

The corresponding optimum pressure of the separator and the boiler is shown in Figure 6.46. The optimum pressure is not a function of the fluid enthalpy, but a function of the reservoir temperature. In this case, the upper limit for the separator pressure is set to 20 bar due to assumed maximum separator pressure. The optimum boiler pressure for brine-powered ORC turbine is restricted to 30 bar, due to the critical temperature of the binary fluid (n-pentane). Similar to the SSBB system, the optimized boiler pressure for a steam-powered ORC turbine is constant at 6.8 bar.

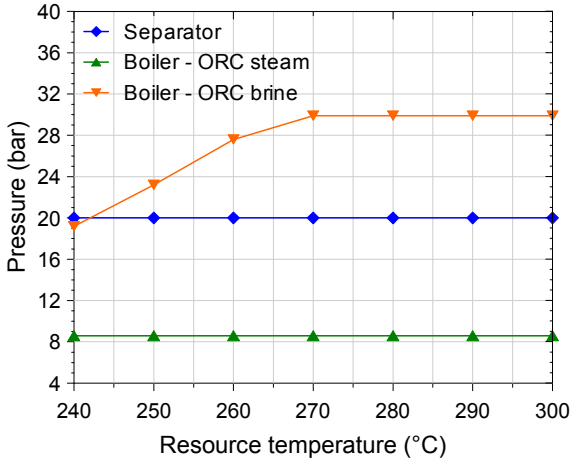

FIGURE 6.46: Optimized boiler and separator pressure for different reservoir temperatures in a hybrid system

The power output from a hybrid system strongly depends on the maximum design separator pressure. This correlation is shown in Figure 6.47. If the wells can supply a high separator pressure, the hybrid system produces high specific power output.

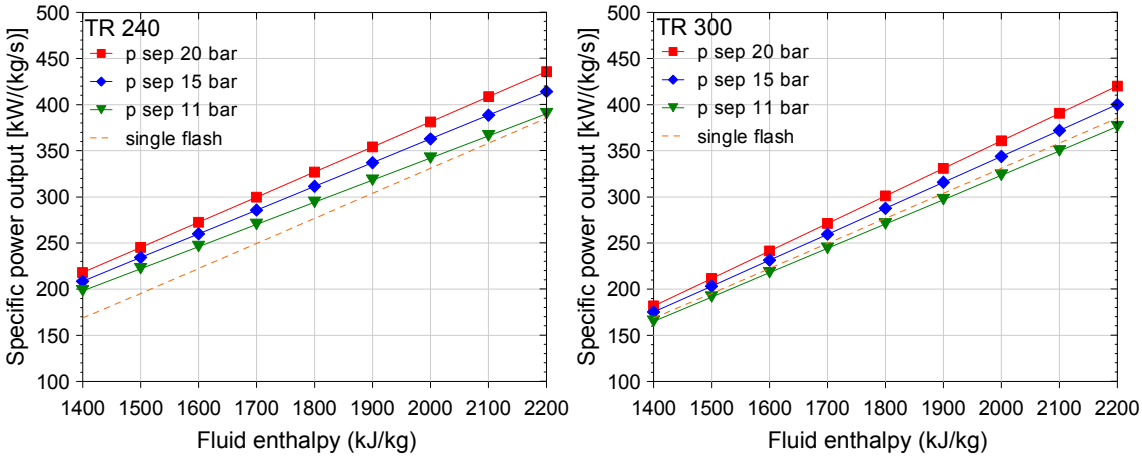

FIGURE 6.47: Specific power output of a hybrid system as a function of fluid enthalpy and maximum separator pressure

Optimized power output from hybrid system as a function of fluid enthalpy for different reservoir temperature is shown in Figure 6.48.

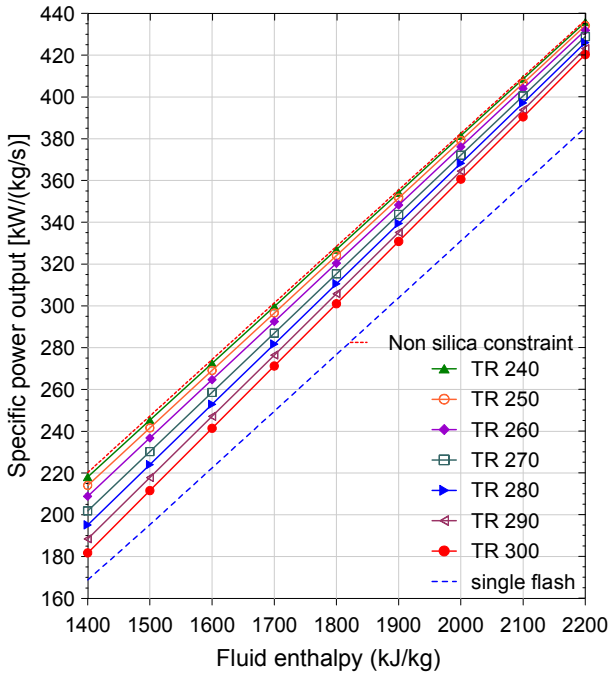

FIGURE 6.48: Optimized specific power output for different reservoir temperatures from a hybrid system

Figure 6.48 shows that the specific power output produced from a hotter reservoir temperature is lower due to the silica scaling constraint. For example, the maximum specific power output produced from a geothermal fluid which has an enthalpy of 1800 kJ/kg at a resource temperature of 300°C is 301 kW/(kg/s), which is 8% lower than for the same fluid at a resource temperature of 240°C (327 kW/(kg/s)). The dashed line (Figure 6.48) represents the single flash specific power output in order to compare it with other systems. For a resource temperature between 240°C and 300°C, the hybrid system gives higher power output than the single flash system.

Figure 6.49 shows that the percentage of additional specific power output in a hybrid system, from a hotter reservoir temperature, is smaller due to the silica scaling constraint. For example, the power output of a hybrid system for a resource temperature of 240°C and fluid enthalpy of 1800 kJ/kg is 18.1% higher than for a single flash system and only 8.7% if the resource temperature is 300°C.

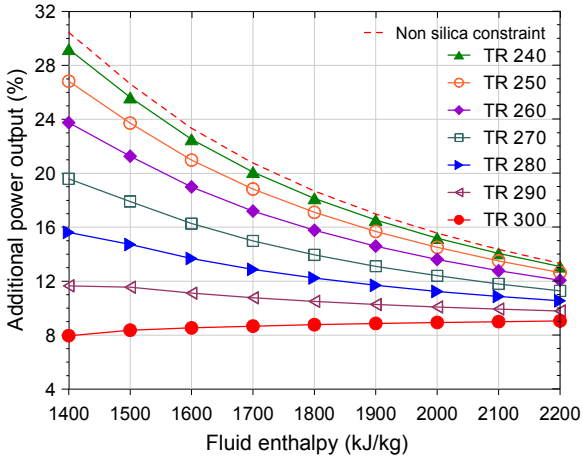

FIGURE 6.49: Percentage of additional specific power output
for different reservoir temperatures in a hybrid system

6.6 Comparison of power cycles

6.6.1 Specific power output comparison between power cycles

Case A (no excess enthalpy wells)
The optimum specific power output from each power cycle is summarized in Figure 6.50 for the case where the geothermal fluid is produced from wells with no-excess enthalpy. The spent steam bottoming binary (SSBB) system has the lowest power production output. The brine bottoming binary (BBB) system and the hybrid system are superior at a certain range of resource temperatures. The order of preference is shown as follows:

- At a range of resource temperatures from 200°C to about 240°C
  brine bottoming binary system > hybrid system > double flash system > spent steam bottoming binary system
- At a range of resource temperatures from 240°C to about 260°C
  hybrid system > brine bottoming binary system > double flash system > spent steam bottoming binary system
- At a range of resource temperatures from 260°C to 300°C
  hybrid system > double flash system > brine bottoming binary system > spent steam bottoming binary system

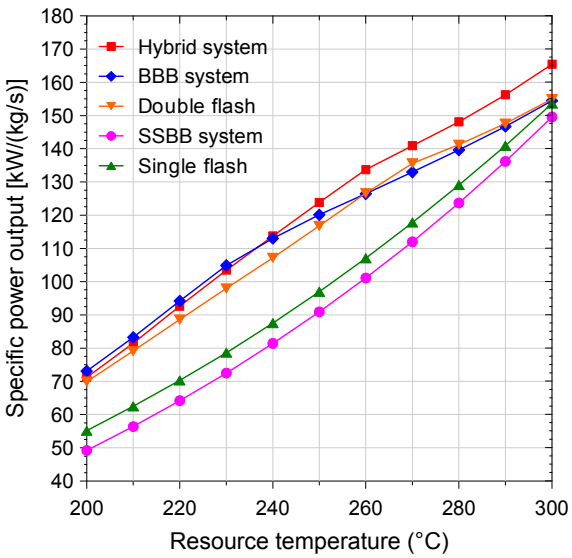

FIGURE 6.50: Comparison of specific power output from different power cycles,
with no-excess enthalpy wells

Figure 6.51 shows the additional specific power output from the different systems, compared to a single flash system.

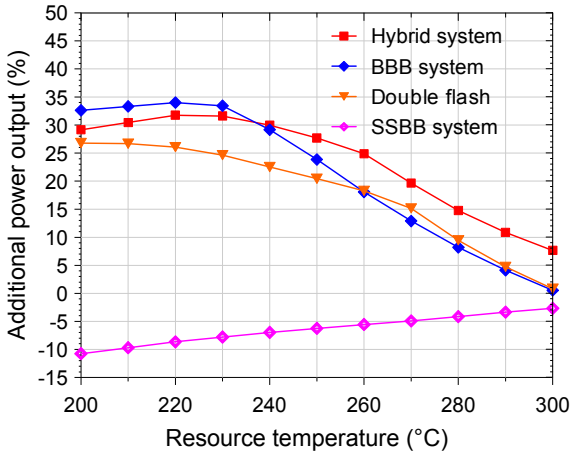

FIGURE 6.51: Percentage of additional specific power output from different power cycles for no-excess enthalpy wells

Figure 6.51 shows that the additional power output percentage from the double flash system, the BBB system and the hybrid system decreases inversely proportional to the resource temperature, due to silica constraint. When the temperature increases the possibility of silica scaling deposition is also high.

The double flash, the BBB system and the hybrid system utilize excess brine from a single flash system to produce additional power output. Thus, the percentage of additional power output from those power cycles will decrease inversely proportionally to the resource temperature. This trend is not seen for the spent steam bottoming binary system because the additional power output comes from a binary turbine which uses steam instead of brine.
The presentation of additional specific power output for different power cycles is shown in Table 6.2.

TABLE 6.2: Percentage of additional specific power output at different resource temperatures

Temperature (°C)	**200**	**210**	**220**	**230**	**240**	**250**	**260**	**270**	**280**	**290**	**300**
Double flash (%)	26.8	26.7	26.1	24.6	22.5	20.4	18.3	15.1	9.4	4.7	0.8
BBB system (%)	32.6	33.3	34.0	33.4	29.2	23.9	18.1	12.9	8.2	4.1	0.5
SSBB system (%)	-10.8	-9.7	-8.7	-7.8	-7.0	-6.2	-5.6	-4.9	-4.2	-3.4	-2.7
Hybrid system (%)	29.2	30.5	31.8	31.6	30.0	27.7	24.9	19.6	14.8	10.9	7.6

The table shows that at a resource temperature of 300°C, the BBB system and the double flash system give additional power output which is less than 1%, while hybrid system gives 7.6% additional power output. For a temperature resource above 300°C, the BBB system and the double flash system cannot be used to increase power output from geothermal resources. Thus, for high-temperature resources, the hybrid system is the most suitable power cycle to be applied.

Case B (excess enthalpy wells)
The optimum specific power output from each power cycle for the case with excess enthalpy is summarized in Figure 6.52.

Figure 6.53 shows the additional specific power output from different systems compared to a single flash system.

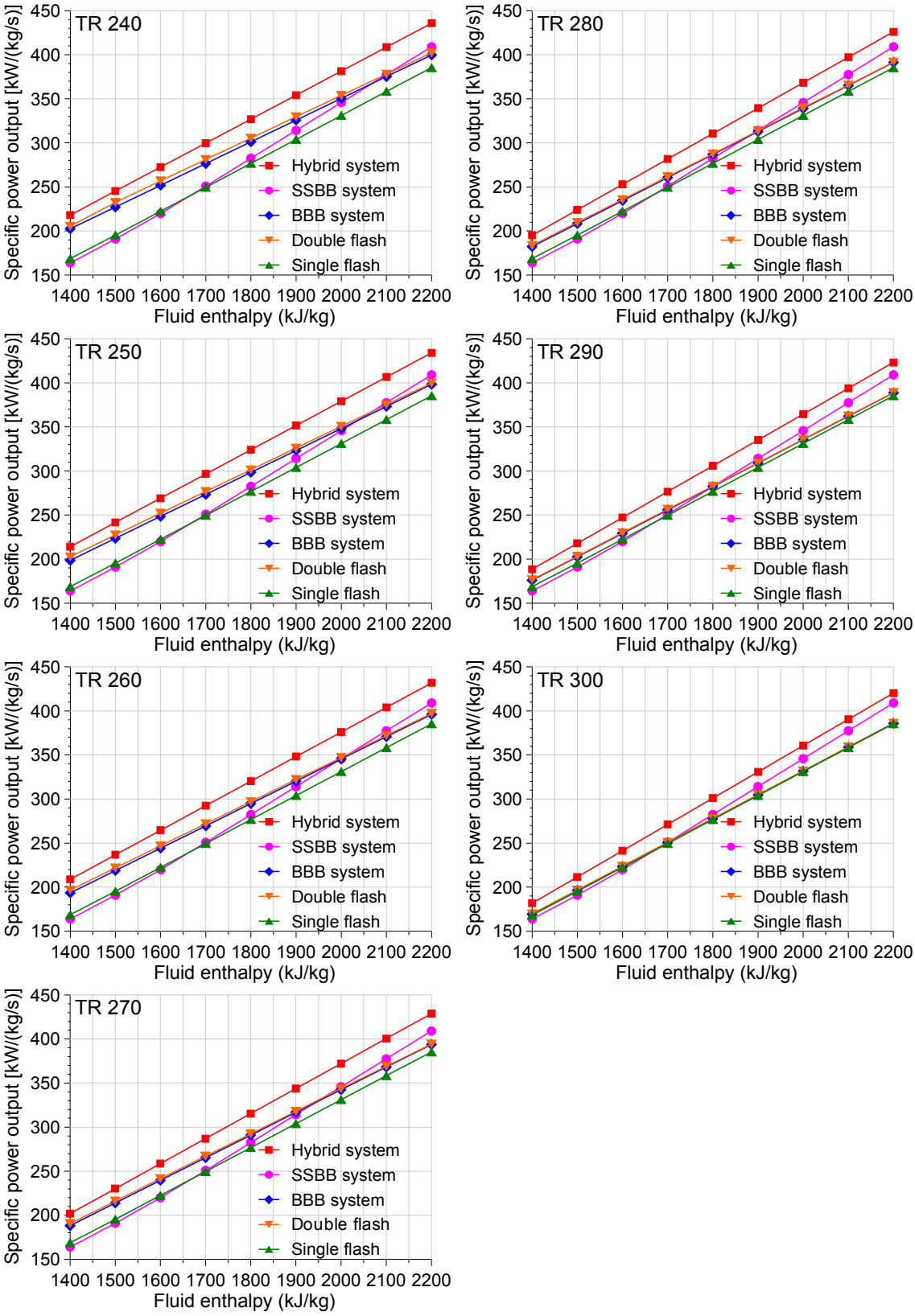

FIGURE 6.52: Comparison of specific power outputs from different power cycles, excess enthalpy case

Figures 6.52 and 6.53 show that:

- Specific power output from a double flash system, a brine bottoming binary (BBB) system and a hybrid system decreases as the fluid enthalpy and the resource temperature increase.

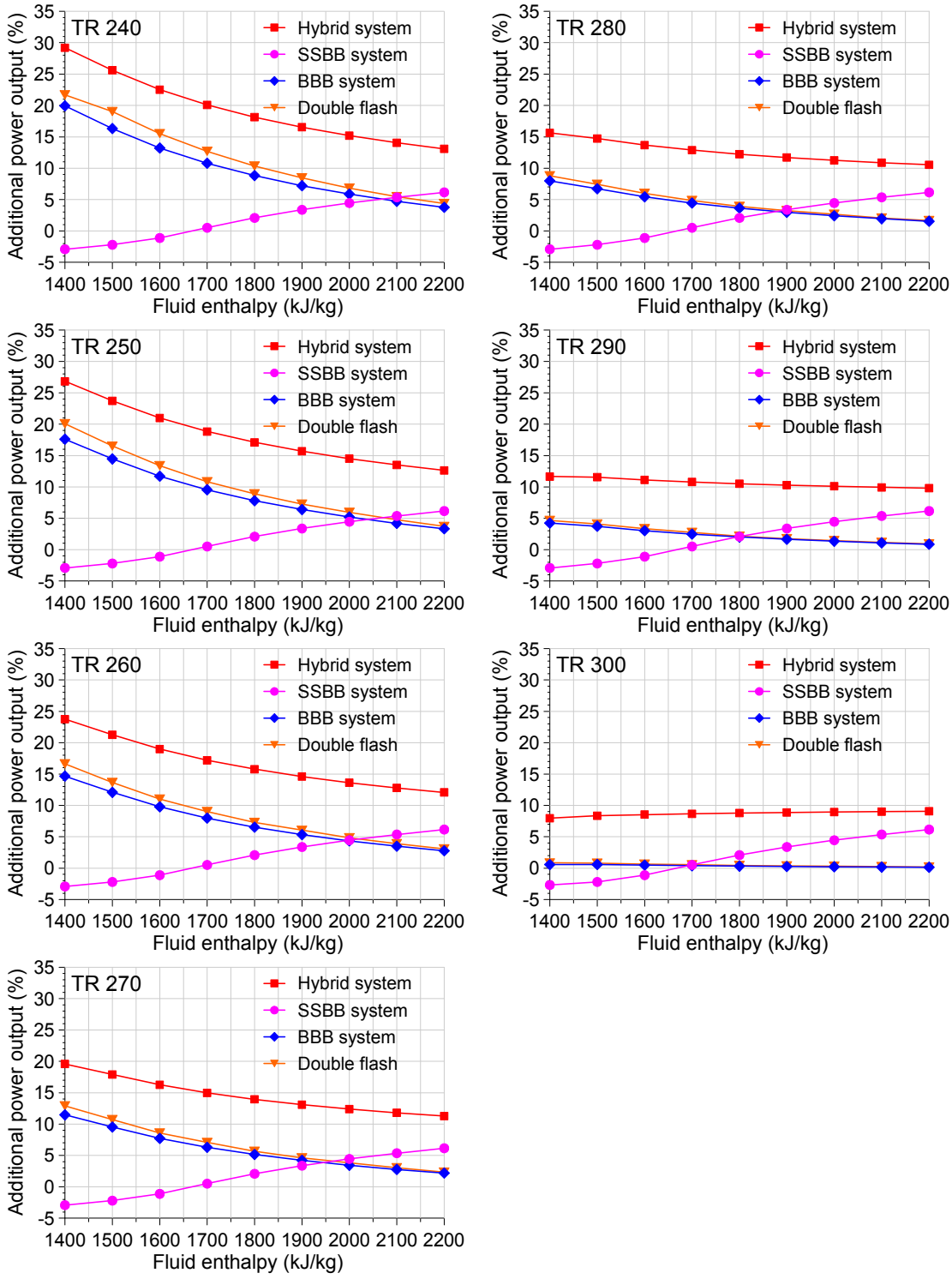

FIGURE 6.53: Percentage of additional specific power output from different power cycles for excess enthalpy case

- The hybrid system is superior to the other plant configurations for all ranges of fluid enthalpy and resource temperatures.
- The double flash system gives higher specific power output compared to the BBB system. The difference reduces with increased fluid enthalpy and the resource temperature.
- At higher fluid enthalpy, the spent steam bottoming binary (SSBB) system starts to exceed both the double flash and brine bottoming binary systems.

6.6.2 Economical comparison between power cycles

A case of 50 MW production was simulated in order to compare the purchased equipment cost and total capital investment for different power plant configurations. The power plant configuration that requires the smallest total investment cost to generate 50 MW from the same resource is the best option.

TABLE 6.3: Breakdown of total capital investment

Cost (x 10^3 US$)	Single flash	Double flash	BBB system	SSBB system	Hybrid system
Steam turbine	46,697	48,997	38,737	14,169	11,492
Standard deviation (Std.) steam turbine	(2,331)	(2,452)	(1,936)	(707)	(574)
Binary turbine	0	0	6,517	18,281	22,198
Std. binary turbine	(0)	(0)	(64)	(179)	(154)
Separator	193	211	142	179	88
Boiler	0	0	1,439	15,441	11,769
Recuperator	0	0	232	0	394
Condenser	3,170	3,101	4,438	2,941	2,778
Pump & compressor	136	134	139	37	67
Cooling tower	1,466	1,446	1,846	1,441	1,784
Total purchased equipment cost (A)	51,662	53,889	53,489	52,488	50,571
Std. PEC	(2,331)	(2,452)	(1,937)	(729)	(594)
Total installation & construction cost (B)	51,662	53,889	53,489	52,488	50,571
Cost of geothermal fluid (C)	37,919	31,153	31,608	39,057	29,348
Std. cost of geothermal fluid	(1,895)	(1,552)	(1,583)	(1,953)	(1,467)
Total capital investment (D) = A + B +	141,242	138,931	138,586	144,033	130,489
Std. total investment cost	(5,035)	(5,140)	(4,182)	(2,438)	(1,888)

For different 50 MW conversion systems, a breakdown of total capital investment for a resource temperature of 240°C and fluid enthalpy of 1400 kJ/kg is shown in Table 6.3. The turbines are the most expensive equipment in the power plants, representing around 22.5-35.3% of the total capital investment. The boiler cost is also significant for the hybrid systems, representing around 9-10.7 % of the total capital investment.

Case A (no excess enthalpy wells)
In the case where the geothermal fluid is producing from wells with no-excess enthalpy, the purchased equipment cost and total capital investment for different power plant configurations and different resource temperatures is shown in Figure 6.54.

The area between the upper and lower lines shows the value ranges for one standard deviation of the uncertain input parameters. The purchased cost of a single flash system has the largest range due to variations in turbine unit cost. The spent steam bottoming binary system is the most expensive option, because it requires a relatively large area for the heat exchangers. The single flash plant requires the smallest purchased equipment cost at low resource temperature, but it is not the best economic option. The single flash system only uses separated steam and, therefore, requires greater mass flow which means more production wells than needed in other power plant configurations. The total investment cost for a single flash system is higher than a double flash system for resource temperatures up to 280°C. The brine bottoming binary (BBB) system requires the lowest total investment cost and is, therefore, the most economically viable option for resource temperatures below 230°C. At higher temperatures, the hybrid system becomes more economically viable.

The presentation of total investment costs for different power cycles is shown in Table 6.4.

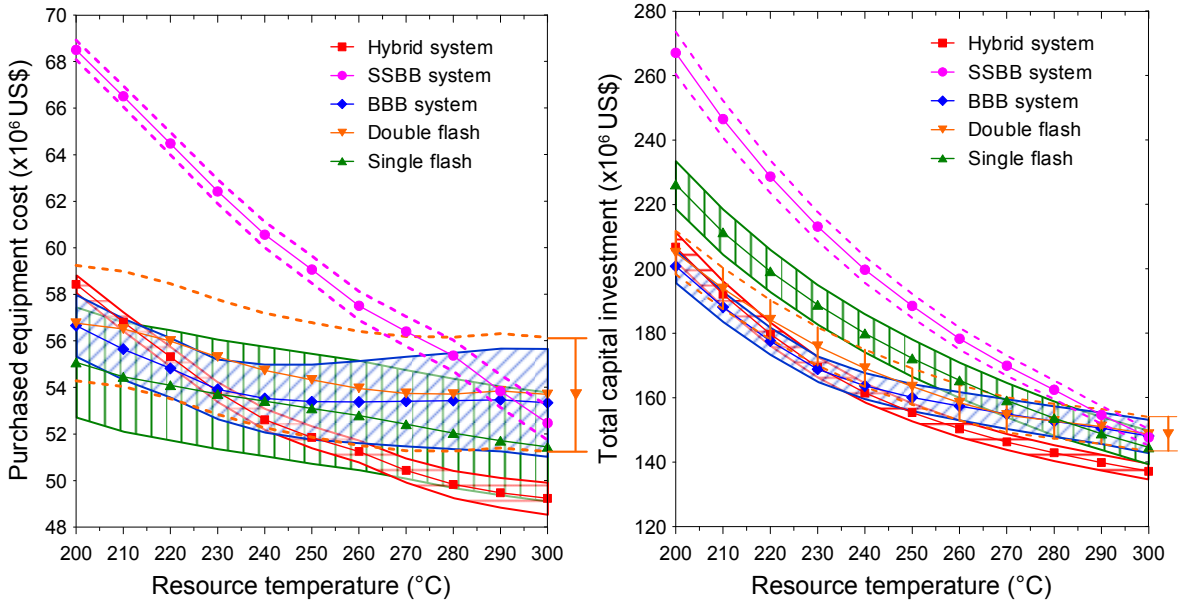

FIGURE 6.54: Purchased equipment cost and total capital investment for different resource temperatures

Table 6.4: Total investment costs for different power cycle at different resource temperatures

Temperature (°C)		200	210	220	230	240	250	260	270	280	290	300
Single flash	AV	226	211	199	189	180	172	165	159	154	149	145
	RV	219-234	204-218	193-206	183-195	174-186	166-178	160-171	154-165	148-159	144-154	139-150
Double flash	AV	205	194	184	176	169	163	158	155	153	151	149
	RV	198-212	188-200	178-190	170-182	163-175	158-169	153-164	149-160	147-158	146-156	143-154
BBB system	AV	201	188	178	169	164	160	157	155	153	151	148
	RV	196-206	183-193	173-182	165-173	160-168	156-164	153-162	150-159	148-157	146-155	143-153
SSBB system	AV	267	246	229	213	200	189	178	170	162	155	148
	RV	261-274	241-252	224-234	209-218	196-204	185-192	175-182	167-173	160-165	152-157	145-150
Hybrid system	AV	207	192	180	169	161	155	150	146	143	140	137
	RV	202-211	188-196	176-183	166-173	159-164	153-158	148-153	144-149	140-145	137-142	135-140

AV = Average Value (x10^6 US$); RV = Range Value within one standard deviation (x10^6 US$)

Case B (excess enthalpy wells)

In the case where the geothermal fluid is produced from wells with excess enthalpy, the purchased equipment cost and total capital investment are shown in Figures 6.55 and 6.56, for different power plant configurations and fluid enthalpies from resource temperatures of 240°C and 300°C. For high fluid enthalpy, the purchased equipment cost for hybrid I and hybrid II becomes lower when compared to the other power cycles. The reason is that those power cycles use back-pressure turbines which are cheaper compared to other systems which use condensing turbines.

Figure 6.56 shows that the total investment cost for a brine bottoming binary (BBB) system and a double flash system is higher for almost the whole range of fluid enthalpies, compared to a single flash system. The trend is more obvious at higher resource temperatures. The hybrid system requires the smallest total investment cost and is, therefore, the most economically viable option for utilizing geothermal fluid at fluid enthalpies below 1700 kJ/kg. At higher fluid enthalpies, a hybrid system requires less mass flow but due to higher total purchased cost for the addition of a bottoming cycle, the total capital investment cost of the spent steam bottoming binary (SSBB) system and hybrid system is similar.

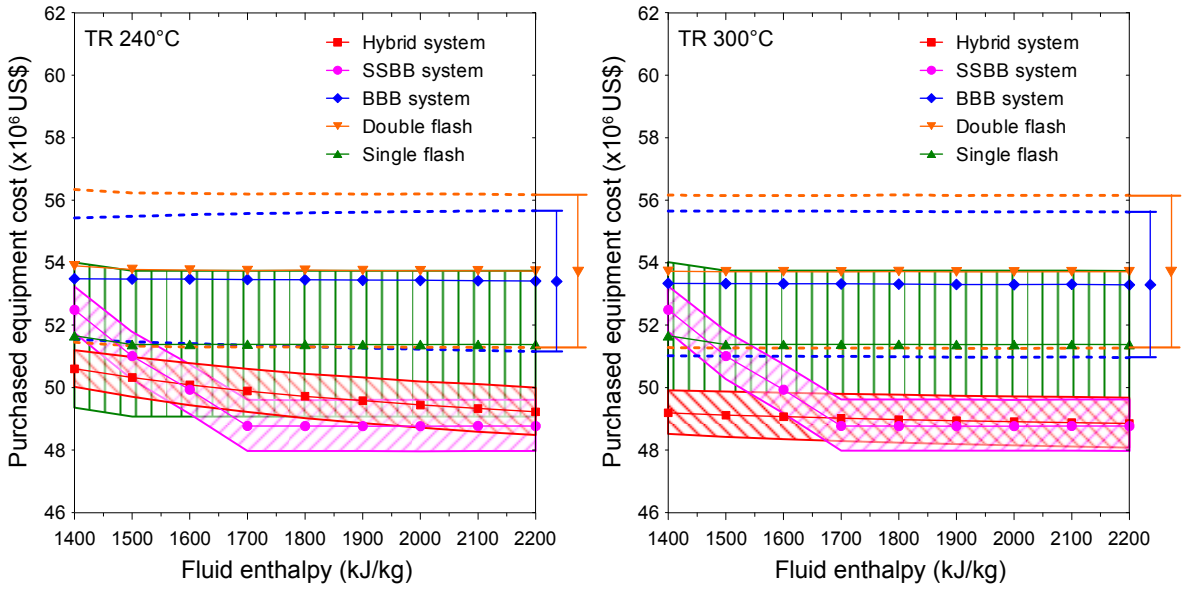

FIGURE 6.55: Purchased equipment cost for different fluid enthalpies at resource temperatures of 240 and 300°C

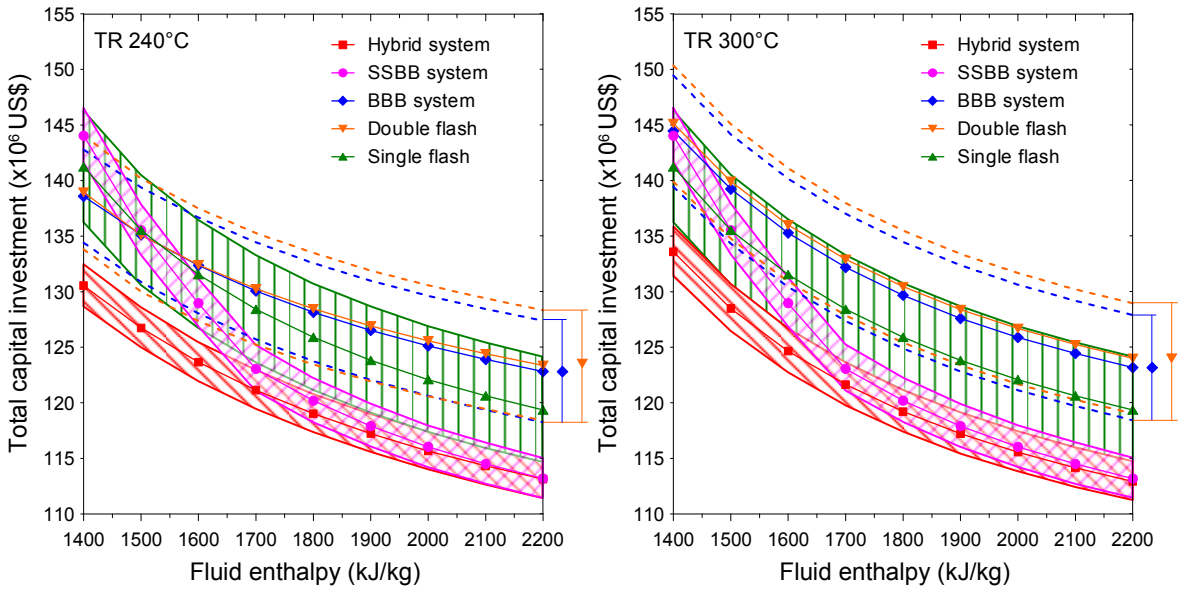

FIGURE 6.56: Total capital investment for different fluid enthalpies at resource temperatures of 240 and 300°C

7. CONCLUSIONS

Utilization of geothermal fluid from high-temperature fields was optimized, using a brine bottoming binary system, a double flash system and a hybrid system as case studies. These systems produced more power output per unit mass flow than a single flash system. The additional power output from these systems depends on the enthalpy of the fluid and the resource temperature. The additional power output decreased inversely proportionally to the fluid enthalpy due to less brine mass fraction used, and also decreased inversely proportionally to the resource temperature due to silica constraints. The effects of silica scaling become significant for resource temperatures above 240°C.

In the case where the geothermal fluid is produced from wells with no-excess enthalpy, for resource temperatures below 240°C, the brine bottoming binary (BBB) system was superior to other types of power plant configurations due to higher specific power output production. Above that temperature, the hybrid system was superior. The BBB system also required the least total investment cost; therefore, it was the most economically viable option for resource temperatures below 230°C. For higher temperatures, the hybrid system became the best economic option.

In the case where the geothermal fluid was produced from wells with excess enthalpy, the hybrid system was superior to other types of power plant configurations due to higher specific power output production. The hybrid system also required the least total investment cost; therefore, it was the most economically viable option for utilizing geothermal fluid at enthalpies below 1700 kJ/kg. At higher fluid enthalpies, the total capital investment cost was similar between the spent steam bottoming binary (SSBB) system and the hybrid system.

The results of this research can be used to determine the optimum expected net power output per unit mass flow as well as its optimum design variables for each type of power plant configuration. The results can also be used to determine which power cycle configuration should be used to maximize the utilization of geothermal fluid from high-temperature fields, for electrical power production based on the characteristics of the fluid and the reservoir.

The main restriction in the economic analysis in this thesis is the lack of recent component prices from the manufacturing companies of power plant components. This financial information is often considered confidential; therefore, in this analysis old published information that was found in the literature was used for the models. The main purpose of the analysis was to compare between different power plant models, so the total costs should be treated as estimates. For decision makers, this thesis could be used as a methodology for comparison between power plant configurations and cost influences. Nevertheless, the component prices must be updated at the moment of decision.

REFERENCES

Arnórsson, S., and Stefánsson, A., 2005: Wet-Steam Well Discharges. II. Assessment of Aquifer Fluid Compositions. *Proceedings of the World Geothermal Congress, 2005, Antalya, Turkey.*

Bandoro Swandaru, R., 2009: *Modelling and optimization of possible bottoming units for general single flash geothermal power plants.* University of Iceland, Reykjavik, MSc thesis.

Bejan A., Tsatsaronis G., and Moran M. 1996: *Thermal design and optimization.* John Wiley & Sons, Inc.,542 pp.

Bronicki, Y.L., 2008: *Advanced power cycles for enhancing geothermal sustainability, 1000 MW deployed worldwide*. IEEE, 2008, 6 pp.

Cooling Tower Depot, Inc., 2010: *Online tool for design, pricing, selection and optimization of cooling tower*. Webpage: *depot.coolingtowerdepot.com/content/depot/cooling-tower-optimization,* accessed on 10 November 2010.

Dipippo, R., 2007: *Geothermal power plants: Principles, applications, case studies and environmental impact* (2nd ed.). Butterworth-Heinemann, 493 pp.

Dipippo, R., 1985: A simplified method for estimating the silica scaling potential in geothermal power plants. *Geothermal Resources Council, Bulletin, May*, 3-9.

Engineering Toolbox, 2010: *Tools and basic information for design, engineering and construction of technical applications*. Webpage: *www.engineeringtoolbox.com/heat-transfer-coefficients-exchangers-d_450.html,* accessed on 20 October 2010.

Environmental Protection Agency (EPA), 2002: *Technology characterization: Steam turbines*. Webpage: *www.uschpa.org/files/public/steamturbines.pdf.*

Geothermal Energy Association (GEA), 2005: *Factors affecting costs of geothermal power development*. August 2005, 12 pp. Webpage: *www.geo-enery.org.*

Grassiani, M., 1999: Siliceous scaling aspects of geothermal power generation using binary cycle heat recovery. *Bulletin d'Hydrogéologie, 17*, 385-392.

Hjartarson, H., 2009: *Waste heat utilization at elkem ferrosilicon plant in Iceland*. University of Iceland, Reykjavik, MSc thesis, 81 pp.

Holman, J. P., 2002: *Heat Transfer* (9th ed.). McGraw-Hill Higher Education.

Jordan, O.T., Borromeo, C.M.R., Reyes, R.L., and Ferrolino, S.R., 2000: A technical and cost assessment of silica deposition in the Palinpinon-I geothermal field, Philippines, over 16 years of production and reinjection. *Proceedings of the World Geothermal Congress, 2000, Japan.*

Karlsdóttir, M.R., 2008: *Utilization of geothermal brine for electrical power production*. University of Iceland, Reykjavik, MSc thesis, 92 pp.

Legmann, H., and Sullivan, P., 2003: The 30 MW Rotokawa I geothermal project five years of operation. *Proceedings International Geothermal Conference, Reykjavik, September, 2003,* 26-31.

Lukawski, M., 2009: *Design and optimization of standardized organic rankine cycle power plant for European conditions*. University of Akureyri, MSc thesis, 76 pp.

Rao, S.R., 1996: *Engineering Optimization: Theory and practice* (3th ed.). John Wiley and Sons, Inc., 922 pp.

Reymann, P., 2000: Stretching the size of geothermal steam turbines. *Proceedings of the World Geothermal Congress 2000, Japan.*

Seider, W.D., Seader, J.D., and Lewin, D.R., 2003: *Product and process design principles* (2nd ed.), John Wiley and Sons, Inc., 802 pp.